Nucleophilic and Electron-Transfer Processes in the Ion-Pair Annihilation of Cationic Iron Complexes (dienyl)$Fe(CO)_3^+$ with $CpMo(CO)_3^-$

R. E. Lehmann and J. K. Kochi*

Department of Chemistry, University of Houston, Houston, Texas 77204-5641

Received April 23, 1990

Spontaneous electron transfer occurs upon the addition of the cationic electrophile (η^5-cyclohexadienyl)$Fe(CO)_3^+$ to the anionic nucleophile $CpMo(CO)_3^-$ in solution to afford the transient 19-electron radical (η^5-cyclohexadienyl)$Fe(CO)_3^\bullet$ and the 17-electron radical $CpMo(CO)_3^\bullet$, which are isolated as the homo dimers [(η^4-cyclohexadiene)$Fe(CO)_3]_2$ and $[CpMo(CO)_3]_2$, respectively, in quantitative yields. Under identical conditions, the open-chain analogue (η^5-hexadienyl)$Fe(CO)_3^+$ leads to the nucleophilic adduct $(OC)_3Fe(\eta^4$-hexadienyl)$Mo(CO)_3Cp$ (**5b**) as the predominant product (75%). The structural characterization of **5b** by X-ray crystallography (monoclinic space group $P2_1/n$ and a = 10.642 (2) Å, b = 7.658 (1) Å, c = 22.440 (4) Å, β = 93.44 (1)°, V = 1825 Å^3, Z = 4, R = 0.025, and R_w = 0.025 for 2435 reflections with $I > 3\sigma$ having $2\theta < 50°$) establishes the nucleophilic addition of $CpMo(CO)_3^-$ to occur at the terminus of the coordinated dienyl ligand. The subsequent thermal decomposition of the nucleophilic adduct proceeds readily at 25 °C by rate-limiting homolysis ($\Delta H^\ddagger \simeq 28$ kcal mol^{-1} and $\Delta S^\ddagger$ = 14 eu) to the radical pair $Fe(CO)_3L^\bullet$ and $CpMo(CO)_3^\bullet$. The overall electron transfer (proceeding as it does via the nucleophilic adduct) is shown to be a general mechanism for the ion-pair annihilation of the cationic dienyliron complexes. This circuitous pathway for electron transfer is discussed in terms of the relatively large intrinsic reorganization energy associated with the reduction of $Fe(CO)_3L^+$ to its 19-electron radical in the outer-sphere mechanism. Such a mechanistic conclusion presents a working format to account generally for the apparent dual pathways that commonly appear as concurrent nucleophilic–electrophilic and electron-transfer processes during the annihilation of organometallic ion pairs.

Introduction

Nucleophilic addition to unsaturated ligands, such as olefins, acetylenes, and arenes coordinated to various metal centers, is a useful strategy in organic synthesis.[1,2] It is especially effective when the organometallic complex is cationic so as to enhance its electrophilic activity.[3] Analogously, the ubiquitous organometallic anions are included among the most potent nucleophiles available.[4] It is thus noteworthy that the ion-pair interaction of such organometallic cations and anions is facile and can successfully lead to the nucleophilic activation of ethylene, acetylene, and benzene;[5] e.g.,

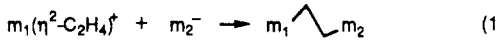

(1)

where m_1 = $CpMo(CO)_3$ and $CpW(CO)_2(PPh_3)$ and m_2 = $CpMo(CO)_3$, $Re(CO)_5$, and $CpW(CO)_2(PPh_3)$.[6]

Many organometallic cations are also readily convertible to 19-electron radicals and, likewise, anions to 17-electron radicals by 1-electron reduction and oxidation, respectively.[7,8] The latter raises the question as to whether the

Table I. Products from the Ion-Pair Annihilation of (η^5-L)$Fe(CO)_3^+$ and $CpMo(CO)_3^-$[a]

L (mmol)	$CpMo(CO)_3^-$, mmol	products (%)[b]
1, pentadienyl (0.46)	0.46	**5a** (95) [47]
2, hexadienyl (0.48)	0.48	**5b** (75) [46]; **7** (25); **6d** (25)
3, cyclohexadienyl (0.73)	0.73	**6a** (95) [75]; **7** (95) [73]
4, cycloheptadienyl (0.08)	0.08	**6b** (c); **7** (90)

[a] Reactions carried out with PF_6^- and PPN^+ salts, respectively, in 10 mL of MeCN or THF at 25 °C. [b] Yields in parenthesis based on stoichiometry in eq 3 or eq 4 by spectral analysis. Isolated yields in brackets. [c] See Experimental Section.

(1) (a) Birch, A. J.; Bandara, B. M. R.; Chamberlain, K.; Chauncey, B.; Dahler, D.; Day, A. I.; Jenkins, I. D.; Kelley, L. F.; Khor, T. C.; Kretschmer, G.; Liepa, A. J.; Narula, A. S.; Raverty, W. D.; Rizzardo, E.; Sell, C.; Strephenson, G. R.; Thompson, D. J.; Williamson, D. H. *Tetrahedron* **1981**, *37*, 289. Birch, A. J.; Pearson, A. J. *Tetrahedron Lett.* **1975**, 2379. (b) Kane-Maguire, L. A. P.; Honig, E. D.; Sweigart, D. A. *Chem. Rev.* **1984**, *84*, 525. (c) Chung, Y. K.; Khoi, H. S.; Sweigart, D. A.; Connelly, N. G. *J. Am. Chem. Soc.* **1982**, *10*, 4245. (d) Faller, J. W.; Chao, K.-H. *Organometallics* **1984**, *3*, 927. (e) Pearson, A. J.; Kole, S. L.; Ray, T. *J. Am. Chem. Soc.* **1984**, *106*, 6060. (f) Van Arsdale, W. E.; Winter, R. E. K.; Kochi, J. K. *J. Organomet. Chem.* **1985**, *296*, 31. (g) Lai, Y.-L.; Tam, W.; Vollhardt, K. P. *J. Organomet. Chem.* **1981**, *216*, 97. (h) Madonik, A. M.; Mandon, D.; Michaud, P.; Lapinte, C.; Astruc, D. *J. Am. Chem. Soc.* **1984**, *106*, 3381.

(2) For reviews, see: (a) Braterman, P. S., Ed. *Reactions of Coordinated Ligands*; Plenum: New York, 1986. (b) Trost, B. M.; Verhoeven, T. R. In *Comprehensive Organometallic Chemistry*; Wilkinson, G., Stone, F. G. A., Abel, E. W., Eds.; Pergamon: New York, 1982; Vol. 8, Chapter 58, p 799ff. (c) Pearson, A. J. *Iden.* Chapter 58, p 939ff. (d) Watts, W. *Iden.* Chapter 59, p 1013ff.

(3) Kochi, J. K. *Organometallic Mechanisms and Catalysis*; Academic: New York, 1978. See also: Alavosus, T. J.; Sweigart, D. A. *J. Am. Chem. Soc.* **1985**, *107*, 985.

(4) (a) King, R. B. *Adv. Organomet. Chem.* **1964**, *2*, 157. (b) Schrauzer, G. N.; Deutsch, E. *J. Am. Chem. Soc.* **1969**, *91*, 3341. (c) For a summary, see: Kochi, J. K. in ref 3, p 156ff.

(5) (a) Beck, W.; Raab, K.; Nagold, U.; Sacher, W. *Angew. Chem.* **1985**, *97*, 498. (b) Beck, W.; Olgemöller, B. *J. Organomet. Chem.* **1977**, *127*, C45. (c) Cameron, A. D.; Laycock, D. E.; Smith, V. H.; Baird, M. C. *J. Chem. Soc., Dalton Trans.* **1987**, 2857. (d) Mueller, H.-J.; Nagel, U.; Beck, W. *Organometallics* **1987**, *6*, 193. (e) Beck, W.; Mueller, H.-J.; Nagel, U. *Angew Chem., Int. Ed. Engl.* **1986**, *25*, 734. (f) Mueller, H.-T.; Beck, W. *J. Organomet. Chem.* **1987**, *330*, C13. (g) Green, M.; Norman, N. C.; Orpen, A. G. *J. Am. Chem. Soc.* **1981**, *103*, 1271. (h) Niemer, B.; Steinmann, M.; Beck, W. *Chem. Ber.* **1988**, *121*, 1767. (i) Beck, W.; Niemer, B.; Wagner, B. *Angew. Chem.* **1989**, *101*, 1699.

(6) (a) Olgemoeller, B.; Beck, W. *Chem. Ber.* **1981**, *114*, 867. (b) Raab, K.; Nagel, U.; Beck, W. *Z. Naturforsch. B* **1983**, *38b*, 1466.

(7) For reviews, see: (a) Chanon, M., Julliard, M., Poite, J. C., Eds. *Paramagnetic Organometallic Species in Activation/Selectivity, Catalysis*; Kluwer: Dordrecht, 1989. (b) Trogler, W. C., Ed. *Organometallic Radical Processes*; Elsevier: New York, 1990.

(8) (a) Dessy, R. E.; Weissmann, P. M. *J. Am. Chem. Soc.* **1966**, *88*, 5124. (b) Kuchynka, D. Y.; Amatore, C.; Kochi, J. K. *Inorg. Chem.* **1986**, *25*, 4087. (c) Dessy, R. E.; King, R. B.; Waldrop, M. *J. Am. Chem. Soc.* **1966**, *88*, 5112.

0276-7333/91/2310-0190$02.50/0

nucleophilic additions to coordinated ligands (L) are actually preceded by an electron-transfer step; i.e.,

$$m_1L^+ + m_2^- \rightarrow \underset{19\text{-e}}{m_1L^\bullet} + \underset{17\text{-e}}{m_2^\bullet}, \quad \text{etc.} \qquad (2)$$

Indeed this mechanistic possibility is supported by sporadic reports of the isolation of dimeric byproducts and other types of evidence of the radical intermediates $m_1L^\bullet$ and $m_2^\bullet$ during the annihilation of organometallic ion pairs.[9,10]

Earlier we described how the structural variability of organometallic cations and anions in their roles as electrophiles and nucleophiles, respectively, can be exploited in establishing the full range of 1-electron (radical) and 2-electron (nucleophilic) processes that stem from reactive ion pairs.[11] This preliminary report is followed here by the detailed comparison of a series of structurally related alkenyliron cations; i.e.,[12,13]

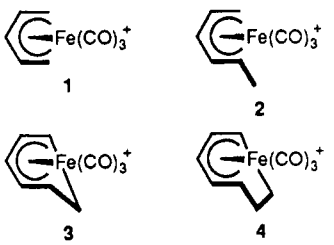

to afford the divergent products stemming from apparently concurrent radical and nucleophilic processes.

Results

In order to optimize the direct comparison of ion-pair reactivities, cations **1–4** were initially treated under a standard set of reaction conditions with a single anionic nucleophile, $CpMo(CO)_3^-$. In each case, $Fe(CO)_3L^+$ as the hexafluorophosphate salt[12,13] was dissolved in acetonitrile and the nucleophilic reagent[14] $PPN^+CpMo(CO)_3^-$ added directly to the pale yellow solution at 25 °C under an argon atmosphere. The reaction mixture immediately turned dark red, and spectral (IR, ^1H NMR) examination within a few minutes, followed by product isolation, revealed the occurrence of two distinctive courses of ion-pair reaction, as described individually below.

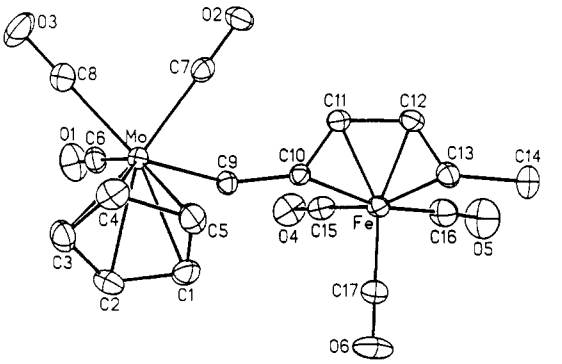

Figure 1. ORTEP diagram of the nucleophilic adduct **5b** from the ion-pair annihilation of (η^5-hexadienyl)$Fe(CO)_3^+$ with $CpMo(CO)_3^-$.

I. Ion-Pair Annihilation to Nucleophilic Adducts. When the pentadienyliron cation **1** was combined with $CpMo(CO)_3^-$ at 25 °C, only a single yellow adduct **5a** was formed in 95% yield, as immediately judged by the growth of the characteristic carbonyl stretching band ν(CO) 2010 cm^{-1} in the IR spectrum.[15] The bright yellow adduct **5a** was also the sole product when a slurry of the pentadienyliron salt, rather insoluble in nonpolar solvents such as dichloromethane or tetrahydrofuran (THF), was treated under otherwise the same reaction conditions (see the full description in the Experimental Section). The homologous hexadienyliron cation **2** was similarly converted to the analogous yellow adduct **5b** with ν(CO) 2012 cm^{-1} as the predominant product[16] (75% yield, Table I). Since the identity of these adducts was critical for the establishment of nucleophilic addition, we deemed it necessary to grow single crystals of the yellow solids from acetonitrile for an unequivocal structure elucidation by X-ray crystallography.

The crystal structure of adduct **5b** was solved in the monoclinic space group $P2_1/n$ by using Patterson techniques to locate the Mo atom and by successive least-squares and difference Fourier calculations to obtain the positions of the other non-hydrogen nuclei. The ORTEP diagram in Figure 1 shows the addition of the $CpMo(CO)_3^-$ nucleophile to have occurred at the methylene terminus of the hexadienyl moiety; i.e.,

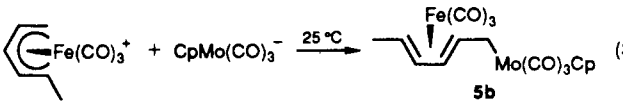

(3)

[The hydrogens attached to the diene are not shown, but they were located in the difference Fourier map.] Importantly, the stereochemical establishment of the *trans,trans*-η^4-hexadiene moiety complexed to $Fe(CO)_3$ in Figure 1 allowed all the hydrogens in the ^1H NMR spectrum of **5b** to be unambiguously assigned, as described in the Experimental Section. Furthermore, the strong similarity of the latter with the ^1H NMR (and IR) spectra of the pentadienyl adduct **5a** established the common pathway for nucleophilic addition of $CpMo(CO)_3^-$ to the pen-

(9) (a) Pearson, A. J.; Yoon, J. *Tetrahedron Lett.* **1985**, *26*, 2399. (b) Reddy, B. R.; Vaughan, V.; McKennis, J. S. *Tetrahedron Lett.* **1980**, *21*, 3639. (c) Moll, M.; Wurstl, P.; Behrens, H.; Marbach, P. *Z. Naturforsch. B* **1978**, *33b*, 1304. (d) Abel, E. W.; Bennett, M. A.; Wilkinson, G. *J. Chem. Soc.* **1985**, 4559. (e) Ciapanelli, D.; Rosenblum, M. *J. Am. Chem. Soc.* **1969**, *91*, 3673. (f) Nesmeyanov, A. N.; Makarova, L. G.; Ustynyuk, N. A. *J. Organomet. Chem.* **1970**, *23*, 517. (g) Treichel, P. M.; Shubkin, R. L. *Inorg. Chem.* **1967**, *6*, 1328. (h) Bonnesen, P. V.; Baker, A. T.; Hersh, W. J. *J. Am. Chem. Soc.* **1986**, *108*, 8304.

(10) (a) Atwood, J. D. *Inorg. Chem.* **1987**, *26*, 2918. (b) Lee, K. Y.; Kuchynka, D. Y.; Kochi, J. K. *Organometallics* **1987**, *6*, 1886. (c) Szabo, P.; Fekete, L.; Bor, G. *J. Organomet. Chem.* **1968**, *12*, 245. (d) Kruck, T.; Hoefler, M. *Chem. Ber.* **1964**, *97*, 2289. (e) Kruck, T.; Hoefler, M.; Noack, M. *Chem. Ber.* **1966**, *99*, 1153. (f) Pearson, A. J.; Kole, S. A.; Ray, T. *J. Am. Chem. Soc.* **1984**, *106*, 6060. (g) Airoldi, M.; Deganello, G.; Dia, G.; Saccone, P.; Takats, J. *Inorg. Chim. Acta* **1980**, *41*, 171. (h) Adams, H.; Bailey, N. A.; Gauntlett, J. T.; Winter, M. J. *J. Chem. Soc., Chem. Commun.* **1984**, 1360. (i) Green, M.; Hughes, R. P. *J. Chem. Soc., Chem. Commun.* **1975**, 862. (j) Van Arsdale, W. E.; Winter, R. E. K.; Kochi, J. K. *Organometallics* **1986**, *5*, 645. (k) Mandon, D.; Astruc, D. *Organometallics* **1989**, *8*, 2372.

(11) Lehmann, R. E.; Bockman, T. M.; Kochi, J. K. *J. Am. Chem. Soc.* **1990**, *112*, 458.

(12) (a) Mahler, J. E.; Pettit, R. *J. Am. Chem. Soc.* **1963**, *85*, 3955. (b) Mahler, J. E.; Gibson, D. H.; Pettit, R. *J. Am. Chem. Soc.* **1963**, 85, 3959. (c) Anderson, M.; Clague, A. D. H.; Blaauw, L. P.; Couperus, P. A. *J. Organomet. Chem.* **1973**, *56*, 307.

(13) (a) Fischer, E. O.; Fischer, R. D. *Angew. Chem.* **1960**, *72*, 919. (b) Dauben, H. J., Jr.; Bertelli, D. J. *J. Am. Chem. Soc.* **1961**, *83*, 497. (c) Birch, A. J. *Org. Synth.* **1979**, *57*, 107.

(14) (a) Abel, E. W.; Singh, A.; Wilkinson, G. *J. Chem. Soc.* **1960**, 1321. (b) Eisch, J. J., King, R. B., Eds. *Organometallic Synthesis*; Academic: New York, 1965; Vol. I, p 114. (c) King, R. B. *Acc. Chem. Res.* **1970**, *3*, 417. (d) Inkrott, P.; Goetze, R.; Shore, S. G. *J. Organomet. Chem.* **1978**, *154*, 337. (e) Hayter, R. G. *Inorg. Chem.* **1963**, 2, 1031.

(15) (a) The first member of this class of compounds, $CpMo(CO)_3CH_3$, has ν(CO) 2020 and 1937 cm^{-1} (CCl_4); see: Cousins, M.; Green, M. L. H. *J. Chem. Soc.* **1963**, 889. (b) Braterman, P. S. *Metal Carbonyl Spectra*; Academic: New York, 1975.

(16) The remainder of the material balance was accounted for (Table I) as a mixture of the iron dimer $[(C_6H_7)Fe(CO)_3]_2$ **6d** and the molybdenum dimer **7** (vide infra).

tadienyl and hexadienyl ligands to occur as in eq 3. Accordingly, the products (**5**) are hereafter designated as *nucleophilic adducts*.

II. Ion-Pair Annihilation to Radical Dimers. Radicals were formed spontaneously upon the addition of $CpMo(CO)_3^-$ to the cyclohexadienyliron cation **3**, as observed spectroscopically at 25 °C by the rapid disappearance of both carbonylmetal ions and the simultaneous formation of the corresponding pair of homo dimers; i.e.,

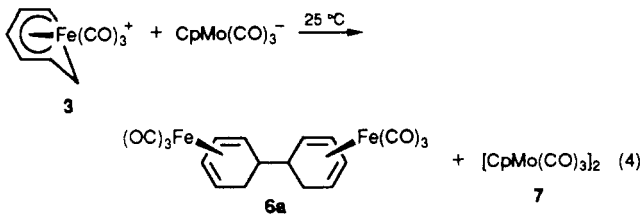

The molybdenum dimer **7** separated from solution as dark purple crystals[17] in essentially quantitative yields. Workup of the reaction mixture afforded similarly high yields (Table I) of the iron dimer **6a**.[18] The formation of the latter was particularly diagnostic, since this unique carbon–carbon-bonded reductive dimer was recently demonstrated by Wrighton and co-workers to arise via the transient 19-electron radical (η^5-cyclohexadienyl)$Fe(CO)_3$• by regiospecific coupling at a ligand center.[19,20] Furthermore, the 17-electron radical $CpMo(CO)_3$• was the precursor to the accompanying oxidative dimer $[CpMo(CO)_3]_2$ (**7**), as described in the earlier anodic studies of $CpMo(CO)_3^-$.[21,22] Accordingly, these products (**6** and **7**) of ion-pair annihilation will be referred to hereafter as *radical (homo) dimers*.

The careful spectral examination of the reaction mixture above at 25 °C provided no evidence in eq 4 for the presence of the nucleophilic adduct analogous to **5a** and **5b**.[23] Similarly, the homologous cycloheptatrienyliron cation **4** yielded only a mixture of the iron dimer [(cycloheptadiene)$Fe(CO)_3]_2$ (**6b**)[24] and the molybdenum dimer **7**[17] in high yields (Table I). The singular absence of a nucleophilic adduct from either **3** or **4** suggested that much milder conditions be employed in the ion-pair annihilation.

A. Isolation of the Labile Intermediate from (cyclohexadienyl)$Fe(CO)_3^+$ Annihilation. When a THF slurry of the cyclohexadienyliron cation **3** was treated at −78 °C with $CpMo(CO)_3^-$, it gradually dissolved to afford a bright yellow mixture. No evidence of the red intermediate that was readily apparent at higher temperatures (vide supra) could be discerned. Instead, after the separation of the accompanying colorless precipitate of $PPN^+PF_6^-$ at −50 °C, the IR spectrum of the chilled solution was found to be essentially identical with that of the nucleophilic adducts (**5**) (vide supra). Upon warming the clear yellow solution to −20 °C, it turned red and deposited dark purple crystals of the molybdenum dimer **7** in essentially quantitative yields, and the accompanying mother liquor also afforded an equimolar amount of the cyclohexadienyliron dimer **6a**; i.e.,

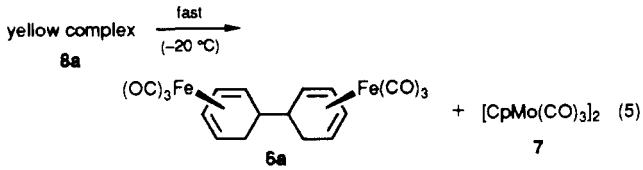

Careful workup of the labile yellow solution by solvent removal in vacuo at −30 °C yielded the thermally unstable, bright yellow complex **8a** in high yields.

B. Nucleophilic Adduct as the Labile Intermediate from Cycloalkadienyliron Cations. Although repeated attempts to grow a single crystal from **8a** for X-ray crystallography were unsuccessful, its spectral properties left little doubt that it be formulated as the nucleophilic adduct that is structurally analogous to **5a** and **5b**. Indeed the formation of the molybdenum and iron dimers **7** and **6a** at −20 °C (eq 5) was consistent with the yellow solid **8a** being a labile intermediate in the ion-pair annihilation; e.g.,

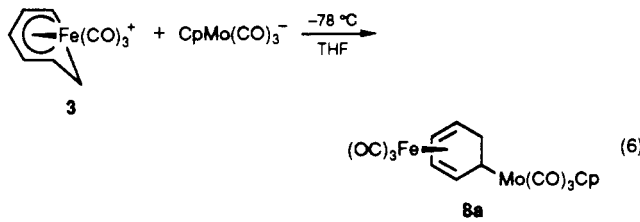

A similar yellow solid **8b** was also obtained when the homologous cycloheptadienyliron cation **4** was treated with $CpMo(CO)_3^-$ at −78 °C. However, we judge from its ready decomposition to an equimolar mixture of the molybdenum and iron dimers **7** and **6b** at −40 °C that **8b** was even less stable than **8a**.[25]

The labile intermediate **8a** was formulated in eq 6 on the basis of its spectroscopic similarity to the authenticated structure (Figure 1) of the nucleophilic adduct **5b**. Thus, the ready homolysis of the labile intermediate in eq 5 raises the parallel question as to the corresponding fate of the nucleophilic adducts.

III. Thermal Decomposition of Nucleophilic Adducts. Solutions of the nucleophilic adducts **5a** and **5b** were thermally unstable and slowly degraded—even at room temperature in the absence of air. Visually, the bright yellow solution of **5b** in hexane gradually darkened merely upon standing in the dark. After several hours, it deposited the insoluble purple crystals of the molybdenum dimer **7** in essentially quantitative yields, and an equimolar amount of the iron dimer **6d**[26] could be isolated from the mother liquor; i.e.,

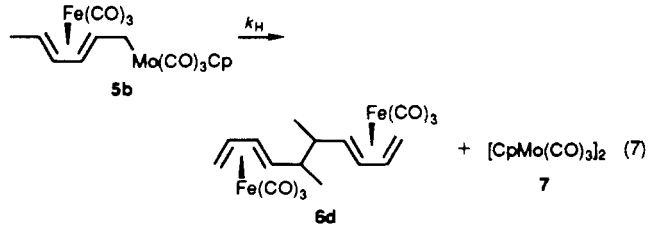

The kinetics of the decomposition were measured in various solvents by simultaneously following the disap-

(17) (a) Piper, T. S.; Wilkinson, G. *J. Inorg. Nucl. Chem.* **1956**, *3*, 104. (b) Lucas, C. R.; Walsh, K. A. *J. Chem. Educ.* **1987**, *64*, 265. See also refs 14b and 15b.

(18) (a) Armstead, J. A.; Cox, D. J.; Davis, R. *J. Organomet. Chem.* **1982**, *236*, 213. (b) Birch, A. J.; Jenkins, I. D.; Liepa, A. J. *Tetrahedron Lett.* **1975**, *21*, 1723.

(19) Zou, C.; Ahmed, K. J.; Wrighton, M. S. *J. Am. Chem. Soc.* **1989**, *111*, 1133.

(20) The cyclohexadieneiron dimer **6a** consisted of an approximate 2:3 mixture of trans/cis isomers similar to that previously obtained.[19]

(21) Lemoine, P.; Giraudeau, A.; Gross, M. *J. Am. Soc., Chem. Commun.* **1980**, 77.

(22) Kadish, K. M.; Lacombe, D. A.; Anderson, J. E. *Inorg. Chem.* **1986**, *25*, 2246.

(23) As judged from the absence of a band with ν(CO) ≃ 2015 cm^{-1} in the IR spectrum (see footnote 15).

(24) In addition to small amounts of $(CO)_3Fe(C_7H_{10})$.

(25) For the comparison of **8a** and **8b**, see the Experimental Section.

(26) See: Mahler, J. E.; Gibson, D. H.; Pettit, R. in ref 12b.

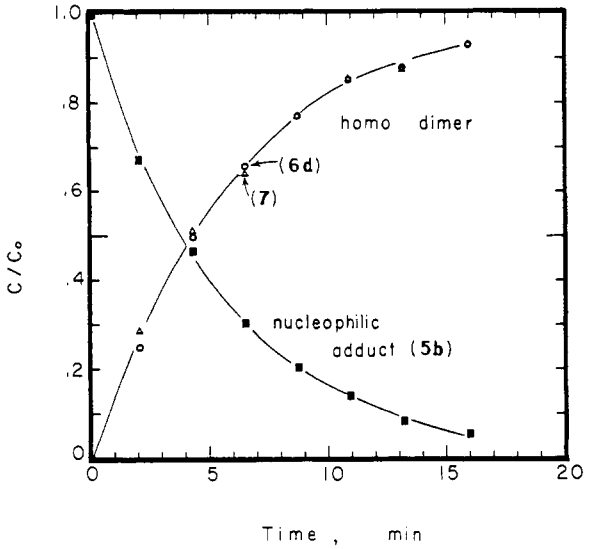

Figure 2. Homolytic decomposition of the nucleophilic adduct **5b** (■) in THF at 50 °C showing the concomitant formation of the homo dimers **6b** (○) and **7** (△).

Table II. First-Order Decomposition of Nucleophilic Adducts[a]

adduct	solvent	temp,[b] °C	$10^5 k_H$,[c] s^{-1}
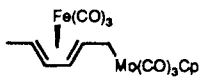 **5b**	CH_3CN	30.0	25.2
	THF	23.0	5.10
		31.7	22.5
		39.8	64.5
		50.0	297
5b	hexane	30.0	32.5
5b	dodecane	30.0	20.2
5b	Nujol	30.0	6.2
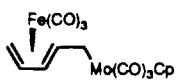 **5a**	THF	50.2	29
		54.8	58
		60.0	133

[a] In solutions containing 6×10^{-3} M nucleophilic adduct. [b] ±0.5 °C. [c] Average of first-order rate constants from the spectral (IR) disappearance of **5** (2015 and 2035 cm^{-1}) and appearance of **6** (2045 cm^{-1}) and **7** (1915 cm^{-1}).

pearance of the nucleophilic adduct and the appearance of the iron and molybdenum dimers by quantitative IR spectrophotometry of their characteristic carbonyl stretching bands, i.e., ν(CO) 2011 (2031), 2044, and 1912 cm^{-1} for **5b**, **6d**, and **7**, respectively, in THF. The typical rates of decomposition of the nucleophilic adduct (**5b**) and concomitant formation of dimeric products (**6d** and **7**) shown in Figure 2 established the stoichiometry according to that in eq 7. Clean first-order kinetics were followed by the decay of the reactant and the growth of both products (see Experimental Section), and the first-order rate constants k_H based on these averaged values evaluated over the course of >3 half-lives are listed in Table II.

The effect of solvent polarity on the first-order decomposition of adduct **5b** is illustrated in Figure 3. Indeed the limited variation (±10%) in the first-order rate constant k_H for thermolyses carried out in media differing as widely as acetonitrile, THF, and hexane underscored the minor role of solvent polarity in adduct decomposition.[27,28]

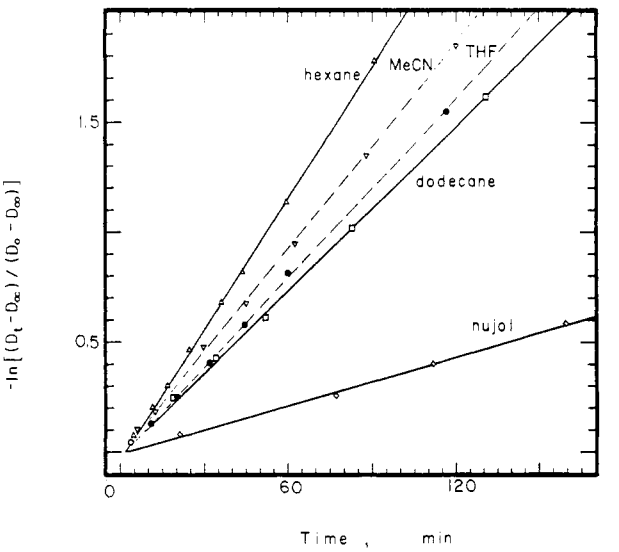

Figure 3. Solvent dependence of the first-order decomposition of the nucleophilic adduct at 30 °C in hexane (△), acetonitrile (▽), THF (●), dodecane (□), and Nujol (○).

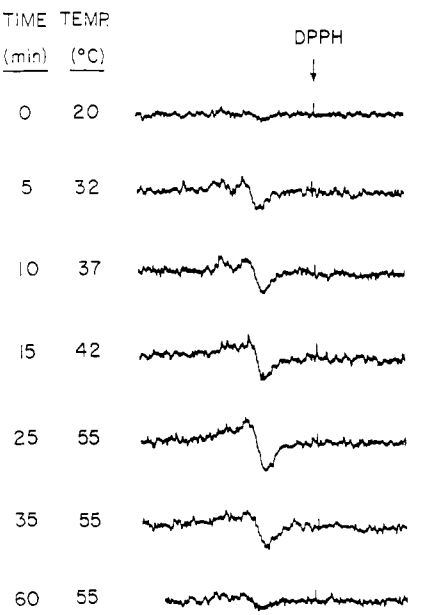

Figure 4. X-band ESR spectra obtained during the decomposition of the nucleophilic adduct **5b** in THF, upon heating as indicated.

Significantly more pronounced in Figure 3 was the effect of solvent viscosity, as indicated by the ~500% decrease in k_H on proceeding from hexane to dodecane to Nujol.[29,30]

From the temperature dependence of the rate constant k_H for decomposition of the hexadiene adduct **5b** in THF solvent between 23 and 50 °C (Table II), the activation parameters were determined as $\Delta H^{\ddagger} = 27.7 \pm 1.6$ kcal mol^{-1} and $\Delta S^{\ddagger} = 14 \pm 5$ cal mol^{-1} K^{-1}. Since the pentadiene adduct **5a** was rather persistent under the same conditions, its clean decomposition to the equimolar mixture of iron dimer[31] **6c** and **7** (compare eq 7) was ex-

(27) For solvent effects on the homolysis of neutral compounds, see: Martin, J. C. In *Free Radicals*; Kochi, J. K., Ed.; Wiley: New York, 1975; Vol. 2, p 493ff.

(28) Compare: (a) Halpern, J. *Acc. Chem. Res.* **1982**, *15*, 238. (b) Geno, M. K.; Halpern, J. *J. Chem. Soc., Chem. Commun.* **1987**, 1052 and references therein.

(29) For the viscosity dependence of homolytic rates of neutral compounds, see: Koenig, T.; Fischer, H. In *Free Radicals*; Kochi, J. K., Ed.; Wiley: New York, 1973; Vol. 2, p 157ff. See also ref 28b.

(30) Typically the viscosities of *n*-hexane, *n*-octadecane, and Nujol are 0.25, 2.77, and 80 cP, respectively. See: Keifer, H.; Traylor, T. G. *J. Am. Chem. Soc.* **1967**, *89*, 1667.

(31) Jotham, R. W.; Kettle, S. F. A.; Moll, D. B.; Stamper, P. J. *J. Organomet. Chem.* **1976**, *118*, 59.

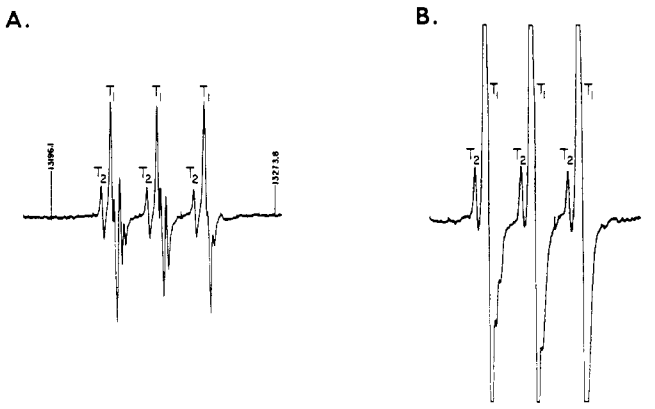

Figure 5. Spin adducts T_1 and T_2 obtained from the nucleophilic adduct **5b** and 2-nitroso-2-methylpropane in THF. (A) ESR spectrum taken after ~15 min at 20 °C. (B) The predominance of T_1 (offscale) at the earliest stage of spin trapping. Additional lines due to small amounts of T_3. ^1H NMR fieldmarkers in kHz.

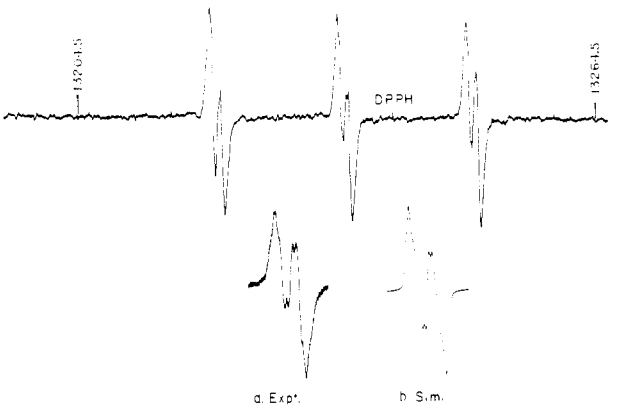

Figure 6. ESR spectrum of the spin adduct T_3 from the nucleophilic adduct **5b** and NB in THF taken 3 h after mixing. Inset a shows the hyperfine splitting of the central nitrogen line, and inset b is the computer simulation with the parameters cited in the text.

amined at slightly elevated temperatures between 50 and 60 °C to afford the activation parameters $\Delta H^{\ddagger} = 31.3 \pm 1.8$ kcal mol^{-1} and $\Delta S^{\ddagger} = 20 \pm 6$ cal mol^{-1} K^{-1}.

A. ESR Spectra and Spin Trapping of Radical Intermediates. The thermolysis of adduct **5b** (as a THF solution in a sealed tube) directly in the cavity of an ESR spectrometer was accompanied by the appearance of an unresolved signal at $\langle g \rangle = 2.044$ and peak width $\Delta H_{pp} \simeq 30$ G. The temporal growth, steady state, and finally decay of the ESR signal for the temperature/time profile in Figure 4 were consistent with transient paramagnetic species as reactive intermediates, i.e.,

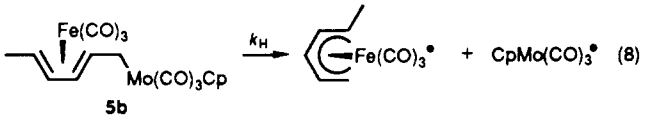

5b

during the decomposition of the nucleophilic adduct according to the stoichiometry in eq 7. Indeed the $\langle g \rangle$ value and peak width are strikingly akin to those previously measured by Wrighton and co-workers for the related radical (η^5-cyclohexadienyl)Fe(CO)$_2$•.[19,32] The corresponding ESR parameters for the highly transient 17-electron radical CpMo(CO)$_3$• are unfortunately not known.[33] However, the thermal decomposition of nucleophilic adduct **5b** in the presence of the free-radical trap 2-nitroso-2-methylpropane (NB)[34] produced transient ESR signals due to a pair of radicals T_1 and T_2 with $\langle g \rangle = 2.007\,45$ and $2.009\,59$, respectively, both showing only nitrogen hyperfine splittings of 16.25 G (Figure 5A).[35] With time, a third more persistent paramagnetic species T_3 with $\langle g \rangle = 2.006\,09$ and $a_N = 14.8$ G gradually appeared with concomitant diminution of both T_1 and T_2 (Figure 5B). The ESR spectrum of T_3 (taken after both T_1 and T_2 had decayed) is shown in Figure 6. Scrutiny of the central ($M_I = 0$) line at high resolution showed further hyperfine splittings (see inset a). Computer simulation of the hyperfine splittings (inset b) was consistent with a methyl quartet of $a_{3H} = 0.26$ G and a pair of singlets with $a_H = 1.15$ and 0.47 G. The latter suggested the following partial structure of T_3,[36] resulting from the homolytic coupling of the spin trap NB at a hexadienyl site.

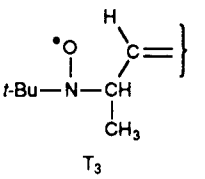

T_3

B. Chemical Trapping of Radical Intermediates. Organometallic radicals such as Fe(CO)$_3$L• and CpMo(CO)$_3$• are known to be reactive in phosphine substitution and halogen transfer.[37] Accordingly, the decomposition of the nucleophilic adduct **5b** was also carried out in THF solutions containing additives such as triphenylphosphine, carbon tetrabromide, and bromoform as well as the spin trap NB (vide supra). In most cases, the products of radical trapping (Table II) were quantitatively identified by their characteristic carbonyl stretching bands in the IR spectra, in comparison with those of known or related structures. For example, the treatment of **5b** with 6 equiv of triphenylphosphine afforded the phosphine-substituted iron[38] and molybdenum[39] dimer, i.e.,

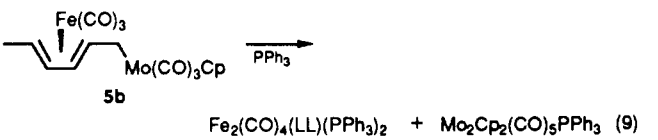

5b

9

with diagnostic IR bands at ν(CO) 1929 (1983) and 1824 (1895, 1972) cm^{-1}, respectively. Minor amounts of the iron and molybdenum homo dimers **6d** and **7** were also observed. It is important to note that **6d** was stable to substitution by PPh_3 and did not afford **9** under the reaction conditions.

(32) These workers reported the weak ESR spectrum as a broad unresolved singlet at $\langle g \rangle = 2.0455$.

(33) For an ambiguous report of CpMo(CO)$_3$•, see ref 21 and the discussion in ref 22. See also: Lindsell, W. E.; Preston, P. N. *J. Chem. Soc., Dalton Trans* **1979**, 1105.

(34) (a) Hudson, A.; Lappert, M. F.; Nicholson, B. K. *J. Chem. Soc., Dalton Trans* **1977**, 551. (b) Forrester, A. R.; Hay, J. M.; Thomson, R. H. *Organic Chemistry of Stable Free Radicals*; Academic: New York, 1968. (c) Rozantsev, E. G. *Free Nitroxy Radicals*; Plenum: New York, 1970.

(35) The ESR spectra of T_1 and T_2 (Figure 5, A and B) are presented in the supplementary material.

(36) For related spin adducts, see: (a) Lagercrantz, C. *J. Phys. Chem.* **1971**, *75*, 3466. (b) Janzen, E. G. *Acc. Chem. Res.* **1971**, *4*, 31.

(37) (a) Herrinton, T. R.; Brown, T. L. *J. Am. Chem. Soc.* **1985**, *107*, 5700. (b) Stiegmann, A. E.; Stieglitz, M.; Tyler, R. D. *J. Am. Chem. Soc.* **1983**, *105*, 6032. (c) Forbus, N.; Brown, T. L. *Inorg. Chem.* **1981**, *20*, 4343. (d) McCullen, S. B.; Brown, T. L. *Inorg. Chem.* **1981**, *20*, 3528. For other examples, see Trogler, W. C. in ref 7b.

(38) Compare with [(η^4-cyclohexadiene)Fe(CO)$_2$PPh$_3$]$_2$ in ref 19.

(39) (a) Haines, R. J.; Nyholm, R. S.; Stiddard, N. H. B. *J. Chem. Soc. A* **1968**, *43*. (b) Barnett, K. W.; Treichel, P. M. *Inorg. Chem.* **1967**, *6*, 294.

Table III. Rates and Products for the Thermal Decomposition of Nucleophilic Adduct 5b in the Presence of Radical Traps[a]

additive (M)	k_H',[b] 10^3 s^{-1}	trapped products (%)[c]
none	0.21	**6d** (95), **7** (90)
$HCCl_3$ (2.1)	0.25	**6d** (96), **7** (92)
CCl_4 (0.11)	1.04	$CpMo(CO)_3Cl$
CCl_4 (2.1)	1.20	$CpMo(CO)_3Cl$
$HCBr_3$ (0.32)	1.24	$CpMo(CO)_3Br$ (*d*)
$HCBr_3$ (0.32)	1.58	$CpMo(CO)_3Br$ (*e*)
$HCBr_3$ (1.6)	1.69	$CpMo(CO)_3Br$ (*e*)
CBr_4 (0.07)	1.62	$CpMo(CO)_3Br$ (*d*)
$(CH_3)_3CNO$ (0.024)	1.08	*d*, **6d** (70)
PPh_3 (0.04)	0.6	**9** (*f*)
PPh_3 (0.18)	0.85	**9** (*f*)

[a] In 5 mL of THF containing 0.03 mmol of **5b** in the dark at 31 °C. [b] First-order kinetics followed by spectral (IR) disappearance of **5b**. [c] By IR analysis, yields in parenthesis. [d] No attempt made to identify product from **5b**. [e] In addition to $(C_6H_9)Fe(CO)_3Br$ in hexane (eq 10), see the Experimental Section. [f] In addition to molybdenum containing product (see eq 9 and the Experimental Section).

The presence of carbon tetrabromide (0.07 M) during the decomposition of **5b** in hexane led to the corresponding bromine-trapped products;[40,41] i.e.,

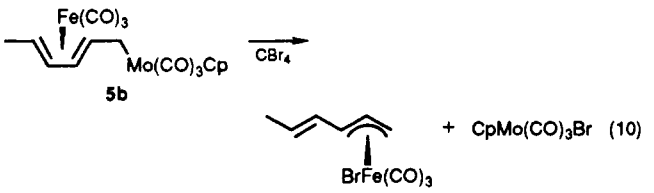

Neither of the homo dimers **6d** or **7** were observed. Bromoform similarly led to the same pair of bromine-substituted iron and molybdenum carbonyls in eq 10. However, the significant amounts of the homo dimer **6d** present among these brominated products suggested that bromoform was not as effective as carbon tetrabromide in bromine-atom transfer to the iron and molybdenum radicals.[42]

The use of excess carbon tetrachloride as the additive resulted in the complete diversion of the molybdenum fragment in **5b** to $CpMo(CO)_3Cl$.[43,44] However, chloroform was an ineffective additive,[45] and the homo dimers **6d** and **7** were the only products formed, even when $CHCl_3$ was present in amounts corresponding to a 700-fold excess.

The spin trap $(CH_3)_3CNO$ efficiently intercepted all the molybdenum radicals from **5b**, since no homo dimer **7** was apparent,[46] even when only 4 M equiv of the NB spin trap was initially present.

The rates of decomposition of the adduct **5b** always maintained first-order kinetics to high conversions, even in the presence of rather high concentrations of additives.

The first-order rate constants k_H' listed in Table III were noteworthy in three ways. First, the values of k_H' were roughly a factor of 4 greater than the k_H values in Table II. Second, they all had about the same magnitude—independent of the chemical nature of the additive. [Chloroform was the sole exception (entry 2) with $k_H' = k_H$, and no trapping products were observed.] Third, the value of k_H' was rather independent of the concentration of the additive (compare CCl_4 in entries 3 and 4).

IV. Spectral Observation at Low Temperatures of the First-Formed Intermediates. In order to examine the earliest stages of ion-pair annihilation, the ^1H NMR spectra of cation/anion pairs were examined at low temperatures. For example, the precooled solutions of (hexadienyl)$Fe(CO)_3^+PF_6^-$ and $PPN^+CpMo(CO)_3^-$ in acetone-d_6 reacted upon mixing at −78 °C to yield a bright yellow solution showing the presence of the single component A, as judged by the digital integration of the well-resolved NMR spectrum arising from one Cp, one methyl, and six inequivalent protons (see the Experimental Section). The latter were particularly diagnostic, since the connectivities in A were readily assigned in the COSY spectrum by exploiting the extensive ^1H–^1H couplings in the alkenyl ligand. Most revealing was the strong spectral similarity of A to the nucleophilic adduct **5b** (Figure 1)—except for those parameters arising from the change in cis/trans configuration at C_2, namely,

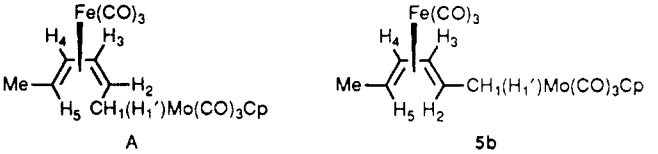

as differences in the vicinal coupling constants of $J_{2,3}$ = 7.2 Hz (A) and 9.3 Hz (**5b**) and chemical shifts of δ H_2 = 3.57 (A) and 2.00 (**5b**).[47]

The spontaneous formation of A with its cis configuration at $C_{2,3}$ clearly represented an initial phase of (hexadienyl)$Fe(CO)_3^+/CpMo(CO)_3^-$ annihilation. The exceptional character of A was manifested in its rapid reaction, even at −25 °C, with 2 equiv of added triphenylphosphine to afford the previously characterized phosphonium salt **10**;[49] i.e.,

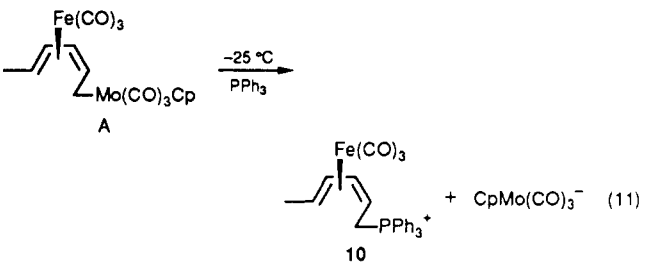

It is important to note that the phosphine substitution in eq 11 to afford the phosphonium salt **10** was tantamount to the *ion-pair reversion* of A, and it thus differed fundamentally from the homolytic cleavage of the trans isomer **5b** to afford the phosphine-substituted dimer **9** in eq 9.

(40) Cheng, C.-C.; Liu, R.-S. *J. Organomet. Chem.* **1986**, *308*, 237.
(41) (a) Sloan, T. E.; Wojcicki, A. *Inorg. Chem.* **1968**, *7*, 1268. (b) Amer, S.; Kramer, G.; Poe, A. *J. Organomet. Chem.* **1981**, *220*, 75.
(42) Similar reactivities have been observed with halogenated methanes: (a) Herrinton, T. R.; Walker, H. W.; Brown, T. L. *Organometallics* **1985**, *4*, 42. (b) Hanckel, J. M.; Lee, K.-W.; Rushmann, P.; Brown, T. L. *Inorg. Chem.* **1986**, *25*, 1852.
(43) (a) Piper, T. S.; Wilkinson, G. *Inorg. Nucl. Chem.* **1956**, *3*, 104. (b) Abrahamson, H. B.; Wrighton, M. S. *J. Am. Chem. Soc.* **1977**, *99*, 5510. (c) Abrahamson, H. B.; Wrighton, M. S. *Inorg. Chem.* **1978**, *17*, 1003.
(44) For the expected (η^3-hexadienyl)$Fe(CO)_3Cl$, see Cheng, C.-C., Liu, R.-S., in ref 40.
(45) In related studies, the relative rates for radical trapping by CCl_4 and $HCCl_3$ were found to be 1000:1 (ref 42a) and 200:1 (ref 42b), respectively.
(46) However, IR analysis indicated the presence of ~70% **6d**. The inefficient trapping of $Fe(CO)_3L^\bullet$ may be attributed to the low concentration of NB.
(47) Further the shift in δ H_5 from 2.99 (A) to 1.47 Hz (**5b**) without an accompanying change in $J_{5,4}$ can be attributed to nonbonded interactions with the Mo center; see ref 48.
(48) (a) Maglio, G.; Palumbo, R. *J. Organomet. Chem.* **1974**, *76*, 367. For the possible effect of the anisotropy of the Mo–Cp fragment, see: (b) Faller, J. W.; Chen, C. C.; Mattina, M. J.; Jakubowski, A. *J. Organomet. Chem.* **1973**, *52*, 361.
(49) (a) McArdle, P.; Sherlock, H. *J. Chem. Soc., Dalton Trans.* **1978**, 1678. (b) Salzer, A.; Hafner, A. *Helv. Chim. Acta* **1983**, *66*, 1774. (c) Evans, J.; Howe, D. V.; Johnson, B. F. G.; Lewis, J. *J. Organomet. Chem.* **1973**, *61*, C48.

The highly labile nature of the first-formed A was also visually apparent in the rapid change of the yellow solution to red upon warming. Shortly at −15 °C, the color change was accompanied in the ^{1}H NMR spectrum of the red solution by the diminution of A and concomitant growth of new resonances due to additional species B and C (see the Experimental Section), together with those of the nucleophilic adduct **5b**, in a relative ratio of ~2:1:1 and 3:1:3 at 50% and 90% conversion of A, respectively. (See the Experimental Section for details.) Finally, when the solution was allowed to thermally equilibrate at room temperature, only **5b** (85%) persisted. Inspection of the IR spectrum revealed the presence of the iron and molybdenum homo dimers **6d** and **7** in the amounts listed in Table I.[50]

These temperature-modulated studies strongly suggested that the transient species B and C were the structural links that connected the initially formed A to the final nucleophilic adduct **5b**. Although they were too labile to isolate as single crystals for X-ray crystallography, the 2-dimensional COSY spectra provided invaluable insight into their structural identity. Thus, the characteristic multiplet patterns for H_1, $H_{1'}$, and H_2 at δ 3.05 (d, J = 13 Hz), 3.35 (d, J = 8 Hz), and 4.10 (ddd, J = 13 × 8 × 8 Hz) in the ^{1}H NMR spectrum of the major species B were diagnostic of a terminal (η^3-allyl)iron group, as previously found in (η^3-pentadienyl)Fe(CO)$_3$Br.[51] The presence of the cis coupling of $J_{2,3}$ = 8.0 Hz and large trans coupling of $J_{4,5}$ = 16 Hz was consistent with the structure

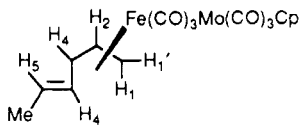

B

(see full analysis in the Experimental Section). Furthermore, the red color (λ_{max} 470 nm, $\epsilon \sim 10^4$ M^{-1} cm^{-1}) was strongly reminiscent of that stemming from the Fe–Mo bonding in the dinuclear complex Cp(CO)$_2$Fe–Mo(CO)$_3$Cp (λ_{max} 400 nm, ϵ = 12 300 M^{-1} cm^{-1}).[52]

The structural identity of the minor species C was also considerably aided by the connectivities revealed in the COSY spectrum—which strongly resembled that of the nucleophilic adduct **5a** (see the Experimental Section). Since the latter is the lower homologue of the structurally characterized **5b**, species C was tentatively assigned the analogous structure below.[53] As such, structure C of the minor intermediate represented the less stable form of the nucleophilic adduct **5b** (see Figure 1).

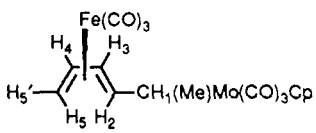

C

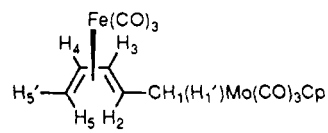

5a

V. Electrochemical Reduction of the Alkenyliron Cations. The electrophilic alkenyliron cations **1**–**4** were evaluated as electron acceptors at a platinum electrode in either THF or acetonitrile solution containing 0.3 or 0.1 M tetra-*n*-butylammonium hexafluorophosphate (TBAH) as the supporting electrolyte. The initial negative-scan cyclic voltammograms (CV) showed well-defined cathodic waves at $E_p^c \sim -0.3$ V vs SCE (Table IV) at 500 mV s^{-1}, but no coupled anodic waves were discerned even at higher scan rates. Such an irreversible CV behavior of Fe(CO)$_3$L$^+$ was similar to that of the related CpFe(CO)$_3^+$ examined earlier[54] and is attributed to the transient character of the 19-electron radical; e.g.,

$$Fe(CO)_3L^+ \xrightarrow{e} Fe(CO)_3L^\bullet \rightarrow Fe(CO)_2L^\bullet + CO \quad (12)$$

Indeed the ready loss of carbon monoxide was also apparent in the cathodic products. For example, the bulk electrolysis of (cycloheptadienyl)Fe(CO)$_3^+$PF$_6^-$ in acetonitrile at a constant potential of −0.5 V consumed 0.97 C to afford an approximately equimolar mixture of the homo (C–C) dimer **6b** and the Fe–Fe dimer **11**,[55] i.e.,

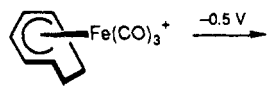

4

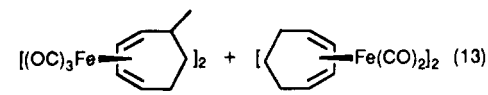

(13)

6b 11

as judged by the appearance of their characteristic carbonyl stretching bands at 2040 and 1756 cm^{-1}, respectively, in the catholyte. Both of these dimers were also apparent in the transient electrochemical experiments by the presence on the return positive CV scan of anodic peaks at E_p^a = 1.12 and 0.67 V, in comparison with those of authentic samples of **6b** and **11**, respectively. Since neither anodic peak was observed on the initial positive CV scan of **4**, they must have arisen via the 19-electron radical—presumably by competition between direct dimerization to **6b**[19] and CO loss[56] followed by dimerization of Fe(CO)$_2$L$^\bullet$ to **11**.[57]

The nucleophilic molybdenum anion CpMo(CO)$_3^-$ can be similarly evaluated as an electron donor by its 1-electron oxidation. The anodic peak potential E_p^a in Table IV was obtained from the irreversible cyclic voltammogram previously measured under the same electrochemical conditions.[22]

Table IV. Electrochemical Parameters for the Reduction of Fe(CO)$_3$L$^+$ and the Oxidation of CpMo(CO)$_3^-$[a]

L	E_p (THF)[b]	E_p (MeCN)[b]
1, η^5-pentadienyl	−0.23	
2, η^5-hexadienyl	−0.26	
3, η^5-cyclohexadienyl	−0.32	−0.45
4, η^5-cycloheptadienyl	−0.35	−0.52
η^5-cyclopentadienyl[c]		−0.41
CpMo(CO)$_3^-$	−0.17[d,e]	−0.06[d,e]
CpMo(CO)$_2$PPh$_3^-$	−0.64[d]	

[a] From cyclic voltammetry at 500 mV s^{-1} in solutions containing 0.3 (THF) or 0.1 (MeCN) M TBAH and 3 × 10^{-3} M substrate. [b] Cathodic peak potential unless stated otherwise. [c] CpFe(CO)$_3^+$ from ref 54. [d] Anodic peak potential. [e] From ref 22.

(50) Note that A was formed uncontaminated with **6d** and **7**. The homo dimers were thus produced during the decomposition of A.

(51) The ^{1}H NMR spectrum of (η^3-pentadienyl)Fe(CO)$_3$Br shows the corresponding resonances for H_1, $H_{1'}$, and H_2 at 3.13, 3.30, and 3.95 ppm, respectively. See ref 40 and the Experimental Section.

(52) Reference 43 and: King, R. B.; Treichel, P. M.; Stone, F. G. A. *Chem. Ind. (London)* **1961**, 747.

(53) Structure C is preferred to the corresponding cis isomer on the basis of the characteristic δ (H_5) = 0.58 ppm. [See ref 48.]

(54) Grant, M. E.; Alexander, J. *J. Coord. Chem.* **1979**, *9*, 205.

(55) Hashmi, M. A.; Munro, J. D.; Pauson, P. L.; Williamson, J. M. *J. Chem. Soc. A* **1967**, 240.

(56) For the facile loss of CO from 19-electron carbonylmetal radicals, see: Narayanan, B. A.; Amatore, C.; Kochi, J. K. *Organometallics* **1986**, *5*, 926. Kuchynka, D. J.; Amatore, C.; Kochi, J. K. *Inorg. Chem.* **1986**, *25*, 4087.

(57) Pending a detailed electrochemical study, the Fe–Fe bonded dimer **11** may also be formed via other (2-electron) pathways.

Scheme I

$$feL^+ + mo^- \xrightarrow{k_N} feLmo \quad (14)$$

Scheme II

$$feL^+ + mo^- \xrightarrow{k_{ET}} feL^\bullet + mo^\bullet \quad (15)$$

$$2feL^\bullet \longrightarrow (feL)_2 \quad (16a)$$

$$2mo^\bullet \longrightarrow mo_2 \quad (16b)$$

Discussion

The alkenyliron cations **1–4** represent an optimum series of electrophiles for the study of nucleophilic interactions as ion pairs since two distinctive processes are clearly delineated, despite minimal changes in reactant structures. Thus, the pentadienyl and hexadienyl derivatives **1** and **2** cleanly yield the nucleophilic adducts **5** whereas the cyclic analogues **3** and **4** yield only the homo dimers **6** according to the stoichiometries in eqs 3 and 4, respectively. Indeed these processes occur *concurrently* in the case of (hexadienyl)$Fe(CO)_3^+$, which in combination with $CpMo(CO)_3^-$ produces both the nucleophilic adduct **5b** in 75% yield together with the homo dimers **6d** and **7** in 25% yields. It is important to emphasize that **5b** is not an intermediate in the formation of **6d** and **7** since its rate of decomposition (eq 7) is much too slow (Table II) to account for the amounts of **6d** and **7** observed (Table I). The foregoing concurrence of pathways from ion-pair interactions indicates that the rate-limiting step leading to nucleophilic addition is highly competitive with that leading to homo dimers. Thus the activation barriers for both processes are closely coupled.

Such divergent products as nucleophilic adducts and homo dimers in eqs 3 and 4 are usually considered to arise via two distinctive pathways. On one hand, the formation of adducts is mostly associated with the direct nucleophilic attack with rate constant k_N at the site of unsaturation on the electrophile in an one-step mechanism, e.g., Scheme I, where fe and mo refer to $Fe(CO)_3$ and $CpMo(CO)_3$, respectively, and L refers to an unsaturated ligand. On the other hand, the homo dimers often derive from a two-step process in which the radical couplings[58] are preceded by electron transfer with rate constant k_{ET}, e.g., Scheme II.

In a more general context, Schemes I and II represent the duality of electrophile/nucleophile interactions that are more commonly described in terms of 2-electron (concerted) and 1-electron (electron-transfer) processes, respectively. However, the rigorous distinction between these apparently disparate processes is more subtle since the homolytic scission of the nucleophilic adduct, i.e.,

$$feLmo \xrightarrow{k_H} feL^\bullet + mo^\bullet \quad (17)$$

affords the pair of radicals leading to the homo dimers in eq 7. The combination of eq 17 with eq 14 is tantamount to the electron transfer in eq 15, or stated alternatively, the activation barrier for electron transfer is equivalent to that for nucleophilic addition as modified by the feL–mo bond energy, i.e., $\log (k_N k_H) \equiv \log k_{ET}$.[59] However, the sizable magnitude of the experimentally determined feL–mo bond energy of $\Delta H \simeq 30$ kcal mol^{-1} (Table II) for the nucleophilic adducts **5** is not consistent with the concurrence of the two pathways (Schemes I and II), which leads to the different conclusion that $\log k_N \simeq \log k_{ET}$ (vide supra). This mechanistic dilemma can be addressed in several ways: (a) rate-limiting electron transfer in Scheme II is a common step leading to nucleophilic adduct, (b) rate-limiting nucleophilic addition in Scheme I is a common step leading to homo dimers, and (c) simultaneous rate-limiting electron transfer and nucleophilic addition are fortuitous. Let us consider each of these possibilities in more detail.

Scheme III

$$feL^+ + mo^- \xrightarrow{k_{ET}} [feL^\bullet, mo^\bullet] \quad (18)$$

$$[feL^\bullet, mo^\bullet] \xrightarrow{k_{cage}} feLmo \quad (19a)$$

$$[feL^\bullet, mo^\bullet] \xrightarrow{k_{diff}} feL^\bullet + mo^\bullet \quad (19b)$$

$$2feL^\bullet \longrightarrow (feL)_2 \quad (20a)$$

$$2mo^\bullet \longrightarrow mo_2 \quad (20b)$$

$$feL^\bullet + mo^\bullet \longrightarrow feLmo \quad (20c)$$

Scheme IV

$$feL^+ + mo^- \xrightarrow{k_N} feLmo \quad (21)$$

$$feLmo \underset{}{\overset{k_H}{\rightleftharpoons}} feL^\bullet + mo^\bullet \quad (22)$$

$$feL^\bullet + mo^\bullet \longrightarrow (feL)_2, mo_2, feLmo \quad (20)$$

(a) *The rate-limiting electron transfer* leading to both nucleophilic adducts and homo dimers formally involves the distinction between the coupling of unlike and like radicals, respectively. Such a mechanism is traditionally formulated as[60] Scheme III, where the brackets denote the solvent cage. According to Scheme III, the competition leading to the nucleophilic adduct and the homo dimers arises largely from the relative rates of cage collapse (k_{cage}) and diffusive separation (k_{diff}) of the radical pair formed as the successor complex in electron transfer in eq 18. Such a formulation, however, is hard pressed to account for the very high selectivity to feLmo shown by cations **1** and **2**—certainly in relation to be structurally related cations **3** and **4**.[61]

(b) *The rate-limiting nucleophilic addition* leading to homo dimers formally includes the reversible homolysis of the nucleophilic adduct,[62] e.g., Scheme IV. Indeed the successful isolation of the labile intermediate **8** from both cyclic cations **3** and **4** indicates that the nucleophilic adduct feLmo is the critical intermediate leading to the homo dimers **6** (compare eq 5 with eq 4). Bond homolysis[63] as the mechanism for the decomposition of the nucleophilic adduct in eq 22 is experimentally supported by the kinetics in Table II and the ESR studies in Figures 4–6, as well as the spin and chemical trapping in Table III. Furthermore,

(58) The rates of many radical couplings are close to diffusion controlled. See ref 36a and: Walker, H. W.; Herrick, R. S.; Olsen, R. J.; Brown, T. L. *Inorg. Chem.* **1984**, *23*, 3748.

(59) By taking the activation free energy and the free energy of formation of the nucleophilic adduct from the ion pair to be roughly the same. The general expression, $\log (K_N k_H) = \log k_{ET}$ is based on K_N, the preequilibrium constant for adduct formation.

(60) See, e.g.: Koenig, T.; Finke, R. G. *J. Am. Chem. Soc.* **1988**, *110*, 2657.

(61) Competition from diffusive separation of the radicals feL$^\bullet$ is expected to be the same owing to their similar structures and molecular weights.

(62) The reversible homolysis in eq 22 actually includes the cage formulation in Scheme III (eq 19). Indeed the competition between cage collapse and diffusive separation in the homolytic decomposition of the nucleophilic adduct is established by the results of chemical trapping in Table III that show the limiting values of $k_{H'} \simeq 4k_H$ to be rather independent of the nature and concentration of the additive. For the kinetics model, see: Noyes, R. M. *J. Am. Chem. Soc.* **1955**, *77*, 2042; **1956**, *78*, 5486; *Prog. React. Kinet.* **1961**, *1*, 129 and ref 60 therein.

(63) For the homolytic cleavage of various organometal bonds, see: Geno, M. K.; Halpern, J. *J. Am. Chem. Soc.* **1987**, *109*, 1238. And: Hay, B. P.; Finke, R. G. *J. Am. Chem. Soc.* **1987**, *109*, 8012 and related papers.

Chart I

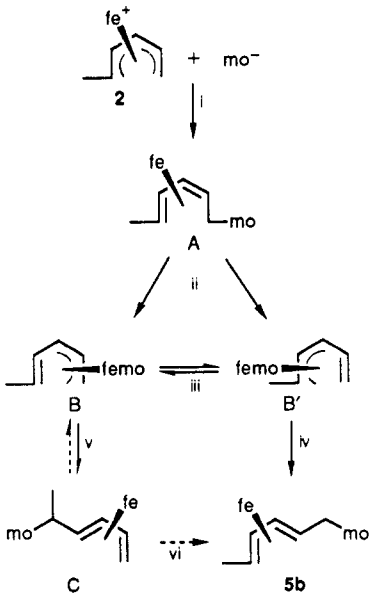

the low sensitivity of the first-order rate constant k_H (Figure 3) on solvent polarity and the marked effect of solvent viscosity (Table II) are both earmarks of the homolytic bond scission.[64]

The mechanism for ion-pair annihilation in Scheme IV taken in a more general context predicts the relative amounts of nucleophilic adduct and homo dimers to be modulated by the homolytic rate constant, i.e., whether k_H is small or large. Such a conclusion requires the high selectivity to derive from a strong dependence of the feL–mo bond strength on the structure of the nucleophilic adduct. Thus, a closer consideration of feLmo structures reveals that the persistent ones (**5a** and **5b**) involve ligand binding to mo at a primary carbon (CH_2) site (see Figure 1), whereas the ligands in the transient feLmo (**8a** and **8b**) can only be bonded to mo at a secondary carbon (>CH) site. The estimated difference in bond energy of ~5 kcal mol^{-1} [65] indeed predicts a half-life to only $\tau \sim 10$ s for **8**[66] relative to the measured value of $\tau = 10^5$ s for **5** (Table II) under the same conditions.[67] Further evidence of this relationship between structure and reactivity is included in the detailed behavior of the cation **2** in the earliest stages of ion-pair annihilation, since the unsymmetrical hexadienyl ligand offers both a primary and a secondary site for nucleophilic attack. Most revealing is the spectral (IR, ^{1}H NMR) observation of the first-formed, highly transient intermediate A at low temperatures, followed by the sequential appearance of metastable species B and C as well as the nucleophilic adduct **5b**. In order to facilitate the presentation, Chart I is included to illustrate how A, B, and C are interrelated as critical intermediates in the conversion of (η^5-hexadienyl)Fe(CO)$_3^+$—with the ligand originally bound to iron in a cis configuration, to the *all-trans*-hexadiene ligand present in the final nucleophilic adduct by a series of a standard organometallic transformations.[68] In Chart I, step i represents ion-pair annihilation by nucleophilic addition to the methylene terminus of the ligand to yield the initially observed intermediate A,[69] which is transformed by a 1,2-shift of mo to the iron center in step ii[70] to generate the fluxional species B and B′ (step iii).[71] In both cases, rotation about the single bond, followed by the retroshift of mo,[72] leads to the nucleophilic adduct **5b** (step iv) and its isomer C (step v). Finally, the disappearance of C upon thermal equilibration at higher temperatures to the more stable adduct **5b** can occur via the reversal of step v. Alternatively, the bond homolysis/recombination in step vi[73] relates intermediate C, with its weak secondary (CH–mo) bond, directly to the labile intermediate 8 (vide supra).

The generalized mechanism for ion-pair annihilation as presented in Scheme IV involves the rather circuitous route for radical-pair production (involving eqs 21 and 22)—certainly in comparison with the electron-transfer pathway (involving only eq 14). In other words, why do ion pairs first make a bond and then break it, when the simple electron transfer directly from anion to cation would achieve the same end? The question thus arises as to whether electron transfer between Fe(CO)$_3$L$^+$ and CpMo(CO)$_3^-$ is energetically disfavored.

The evaluation of the driving force for the electron-transfer process is obtained from the separate redox couples; i.e.,

$$feL^+ + e \underset{}{\overset{E^0_{red}}{\rightleftharpoons}} feL^\bullet \qquad (23)$$

$$mo^- \overset{E^0_{ox}}{\rightleftharpoons} mo^\bullet + e \qquad (24)$$

The overall driving forces for electron transfer $-\Delta G_{ET} = \mathcal{F}(E^0_{red} + E^0_{ox})$ for ion-pair annihilation in THF between mo$^-$ and feL$^+$ (i.e., cations **1**–**4**) are ΔG_{ET} = 3.2, 3.9, 5.3, and 6.0 kcal mol^{-1}, respectively, based on the electrochemical measurements in Table IV.[74,75] Such driving forces all easily lie within the isoergonic bounds for the facile electron transfer between feL$^+$ and mo$^-$.[76] Moreover, the differences in driving forces are not sufficient to strongly distinguish cations **1** and **2** from their cyclic analogues **3** and **4** for the consideration of *simultaneous nucleophilic addition and electron transfer*, as presented in possibility (c) above. We are thus left with the inescapable conclusion that nucleophilic addition is the favored process for the ion-pair annihilation of feL$^+$ and mo$^-$, despite the favorable driving force for electron transfer. Some of the factors that discourage the latter may be related to the large intrinsic reorganization energy required to convert the organometallic cation (feL$^+$) to the corresponding 19-electron radical (feL$^\bullet$).[77] Thus, the facile

(64) See the discussions included in footnotes 27–30.
(65) Average values estimated from the compilation by: Halpern, J. *Bull. Chem. Soc. Jpn.* **1988**, *61*, 13.
(66) Assuming the same preexponential factor.
(67) In solution at room temperature.
(68) Atwood, J. D. *Inorganic and Organometallic Reaction Mechanisms*; Brooks/Cole: Monterey, CA, 1985.
(69) The ^{1}H NMR spectrum at −40 °C showed no indication of paramagnetic line broadening.
(70) A non-ionic pathway was suggested by the low rate dependence on solvent polarity (acetonitrile versus THF/pentane). The driving force for the rearrangement may be attributed to the relief of steric strain of the molybdenum group in the anti configuration (compare footnote 47).
(71) Compare the fluxional behavior of (η^3-cycloheptatrienyl)Fe(CO)$_3^-$ reported by: Maltz, H.; Kelley, B. A. *J. Chem. Soc., Chem. Commun.* **1971**, 1390. And: Li Shing Man, L. K. K.; Takats, J. *J. Organomet. Chem.* **1976**, *117*, C104.
(72) To represent the microscopic reverse process to step (ii).
(73) Such a mechanism represents the cage collapse of the radical pair (compare eq 18a). The extent to which diffusive separation is competitive leads to homo dimers.
(74) Based on the expression[75] $(E_p - E^0)_i = RT/3\mathcal{F}[\ln (k_i C_i RT)/(v\mathcal{F}) - 3.12]$ and $k_{feL} = 10^7$ M^{-1} s^{-1} and $k_{mo} = 2 \times 10^9$ M^{-1} s^{-1} (Hughey, J. L.; Bock, C. R.; Meyer, T. J. *J. Am. Chem. Soc.* **1975**, *97*, 4440), v = 500 mV s^{-1}, and $C_i = 3 \times 10^{-3}$ M.
(75) Olmstead, M. L.; Hamilton, R. G.; Nicholson, R. S. *Anal. Chem.* **1969**, *41*, 260.
(76) For example, electron transfer between the ion pair CpMo(CO)$_3^-$ and various pyridinium salts occurs spontaneously under the same conditions, despite endergonic driving forces ($-\Delta G$) of ~−7 kcal mol^{-1}. Bockman, T. M. Unpublished results.

self-reaction of feL• to couple only at the ligand site[78] suggests that electron transfer to feL$^+$ is accompanied by a large ligand reorganization[79] to place the spin density at a terminal carbon. The "slippage" of the unsaturated ligand would lead to a 17-electron radical,[80] e.g.,

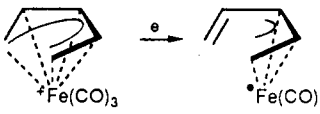

(25)

Such a change in ligand hapticity is probably a general problem associated with the supersaturated nature of 19-electron radicals.[81] In the context of Marcus theory,[82] the sizable barrier for outer-sphere electron transfer posed by a large reorganization energy may be circumvented by a configurational change to favor an inner-sphere activated complex.[83] In the latter regard, the distinction between nucleophilic addition and inner-sphere electron transfer is sufficiently blurred to obscure any further meaningful mechanistic insight into ion-pair annihilation.[84,85]

Experimental Section

Materials. $Fe(CO)_5$ (Alpha) was vacuum distilled prior to use; $Mo(CO)_6$ (Pressure Chemicals), *trans*-pentadienoic acid (Fluka), *trans,trans*-2,4-hexadien-1-ol (Aldrich), 1-methoxy-1,3-cyclohexadiene (Aldrich) and dicyclopentadiene (Aldrich) were used as received. All manipulations were carried out under an argon atmosphere.

Pentane (Mallinckrodt, reagent) and *n*-hexane (Mallinckrodt, reagent) were distilled from sodium. Tetrahydrofuran (THF, Fisher) and diethyl ether (Fisher) were distilled from a mixture of sodium and benzophenone. Dichloromethane (Mallinckrodt) was distilled from P_2O_5 and redistilled from CaH_2. Acetonitrile (Mallinckrodt) was allowed to stand with 0.1% $KMnO_4$ overnight, and the solution was refluxed for 1 h. The brown MnO_2 residue was removed by filtration, and the acetonitrile was fractionally distilled from P_2O_5 and then redistilled from CaH_2. Nitromethane (Fisher, 96%) was fractionally recrystallized three times from a partially frozen mixture at −78 °C. The resulting nitromethane was treated with $CaCl_2$ and fractionally distilled in vacuo at 150 mmHg. Dodecane (Aldrich) was distilled under reduced pressure from sodium. Paraffin oil (Nujol, Fisher) was degassed in vacuo at 60 °C for 4 h.

The iron salts (η^5-L)$Fe(CO)_3^+PF_6^-$ were synthesized according to the procedures described in the literature, viz., **1** (L = pentadienyl) and **2** (L = hexadienyl) were obtained from the reaction of *trans*-2,4-pentadien-1-ol or *trans,trans*-2,4-hexadien-1-ol with triiron dodecacarbonyl,[86] followed by salt formation by the method of Pettit and co-workers.[13] The homologue **3** (L = cyclohexadienyl) was prepared in the same way, but starting with 1-methoxy-1,3-cyclohexadiene and $Fe(CO)_5$,[1a] and **4** (L = cycloheptadienyl) was prepared from cycloheptatriene and $Fe(CO)_5$,[87] followed by treatment with HPF_6.[55] (Di-η^5-cycloheptadienyl)diiron tetracarbonyl (**11**) was also prepared as described.[55]

$[CpMo(CO)_3]_2$ was prepared by the procedure reported by King,[14b] $PPN^+CpMo(CO)_3^-$[14e] was prepared by reduction of $[CpMo(CO)_3]_2$ in THF with 1% sodioamalgam,[14d] followed by metathesis with PPN^+Cl^- (Alfa) and recrystallization from THF. For analytical purposes, the IR data [ν(CO), cm^{-1}] of the relevant carbonylmetal compounds (solvent) were as follows: **1** (CH_3CN) 2120 (s), 2074 (s); **2** (CH_3CN) 2118 (s), 2074 (s); **3** (CH_3CN) 2115 (s), 2068 (s); **4** (CH_3CN), 2112 (s), 2065 (s); **7** (THF) 2012 (w), 1956 (s), 1912 (s, br); **11** (THF) 1983 (s), 1952 (w), 1765 (s); $PPN^+CpMo(CO)_3^-$ (THF) 1898 (s), 1782 (vs).

Instrumentation. NMR spectra were recorded on either a 90-MHz JOEL FX90Q or a 300-MHz GE QE-300 spectrometer. Chemical shifts (δ) are reported in ppm downfield from TMS as the internal standard. Infrared spectra were measured on a Nicolet 10 DX FT-IR spectrometer, equipped with a SPECAC P/N 21500 variable-temperature unit. UV–vis spectra were recorded on a Hewlett-Packard 8450-A diode-array spectrophotometer. Cyclic voltammetry was carried out as described previously.[88] ESR measurements were performed on a Varian E-112 X-band spectrometer with 100-kHz modulation using the perylene cation radical with g = 2.000 214 as the field marker.

***trans*-1-(CpMo(CO)$_3$)(η^4-2,4-pentadiene)Fe(CO)$_3$ (5a).** To $PPN^+CpMo(CO)_3^-$ (362 mg, 0.46 mmol) in 10 mL of acetonitrile at room temperature was added (η^5-pentadienyl)$Fe(CO)_3^+PF_6^-$, **1** (164 mg, 0.46 mmol). The initial dark red color slowly faded. After 5 min, the orange solution was cooled to −20 °C for 24 h. The yellow needles were filtered and recrystallized from 10 mL of acetonitrile by cooling to −20 °C for 36 h. Filtration followed by washing with 2 × 1 mL of cold acetonitrile and drying gave 99 mg of **5a** (0.22 mmol, 47%). Anal. Calcd for $C_{16}H_{12}O_6FeMo$: C, 42.51; H, 2.68. Found: C, 42.54; H, 2.71. IR (hexane): ν(CO) 2043 (s), 2019 (vs), 1973 (vs), 1966 (sh), 1947 (s), 1937 (s) cm^{-1}. ^1H NMR (300 MHz, nitromethane-d_3): δ 5.55–5.54 (m, 1 H, H_3), 5.48 (s, 5 H, Cp), 5.26 (dddd, 1 H, H_4), 2.44 (dd, 1 H, $H_{1'}$), 1.99 (dddd, 1 H, H_2), 1.82 (dd, 1 H, $H_{5'}$), 1.74 (ddd, 1 H, H_1), 0.52 (ddd, 1 H, H_5); $J_{1,1'}$ = 9.3, $J_{1,2}$ = 12.3, $J_{1',2}$ = 3.0, $J_{2,3}$ = 9.2, $J_{2,4}$ = 1.0, $J_{3,4}$ = 5.0, $J_{3,5}$ = 1.0, $J_{3,5'}$ = 1.0, $J_{4,5}$ = 9.4, $J_{4,5'}$ = 7.0, $J_{5,5'}$ = 2.2 Hz.

***trans,trans*-1-(CpMo(CO)$_3$)(η^4-2,4-hexadiene)Fe(CO)$_3$ (5b).** A suspension of $PPN^+CpMo(CO)_3^-$ (377 mg, 0.48 mmol) and (η^5-2,4-hexadien-1-yl)$Fe(CO)_3^+PF_6^-$, **2** (176 mg, 0.48 mmol), in 5 mL of THF in an ice bath was stirred for 1 h. The solvent was evaporated in vacuo at 0 °C and the brown residue extracted with 120 mL of ice-cold hexane. Evaporation of solvent at ≤0 °C affords an orange solid that was recrystallized twice from 10 mL of acetonitrile by cooling the (quickly filtered) solution to −20 °C for 24 h. Yield: 102 mg of **5b**, as yellow crystals (0.22 mmol, 46%). Anal. Calcd for $C_{17}H_{14}O_6FeMo$: C, 43.81; H, 3.03. Found: C, 43.83; H, 3.04. IR (hexane): ν(CO) 2037 (s), 2018 (vs), 1968 (vs), 1946 (s), 1937 (s) cm^{-1}. ^1H NMR (300 MHz, nitromethane-d_3): δ 5.49 (s, 5 H, Cp), 5.30 (dd, 1 H, H_3), 5.07 (m, 1 H, H_4), 2.42 (dd, 1 H, $H_{1'}$), 1.95 (dddd, 1 H, H_2), 1.78 (dd, 1 H, H_1), 1.43–1.33 (m, 4 H, H_5 and Me); $J_{1,1'}$ = 9.3, $J_{1,2}$ = 12.2, $J_{1',2}$ = 3.0, $J_{2,3}$ = 9.3, $J_{2,4}$ = 1.0, $J_{3,4}$ = 5.0, $J_{4,5}$ = 9.4 Hz.

Reaction between (η^5-cyclohexadienyl)Fe(CO)$_3^+$PF$_6^-$, 3, and PPN$^+$CpMo(CO)$_3^-$. A suspension of (η^5-cyclohexadienyl)-$Fe(CO)_3^+PF_6^-$, **3** (265 mg, 0.727 mmol), in 10 mL of THF at room temperature was treated with $PPN^+CpMo(CO)_3^-$ (570 mg, 0.727 mmol). The purple mixture was stirred for 15 min and evaporated to dryness in vacuo. The purple residue was extracted with 2 × 20 mL of hexane. Fractional crystallization at −20 °C for 48 h

(77) For the effect or reorganization energy on the electron-transfer rates of organometals, see Table VI in: Klingler, R. J.; Kochi, J. K. *J. Am. Chem. Soc.* **1981**, *103*, 5846.
(78) See Zou, C.; Ahmed, K. J.; Wrighton, M. S. in ref 19.
(79) To include changes in the metal coordination and the bond lengths of $Fe(CO)_3L^+$. The corresponding changes for $CpMo(CO)_3^-$ are expected to be small.
(80) Such a decrease in ligand coordination accompanying one-electron reduction of iron carbonyls has been noted in the ESR studies of the related (diene)$Fe(CO)_3$ by: Krusic, P. J.; San Filippo, J., Jr. *J. Am. Chem. Soc.* **1982**, *104*, 2645. For analogous changes in ligand hapticity accompanying the reduction of arene–metal complexes, see: Bowyer, W. J.; Merkert, J. W.; Geiger, W. E.; Rheingold, A. L. *Organometallics* **1989**, *8*, 191.
(81) (a) For the highly labile nature of 19-electron radicals, see: Kuchynka, D. J.; Kochi, J. K. *Inorg. Chem.* **1989**, *28*, 855. And Trogler, W. C. in ref 7b. (b) If so, the corresponding 17-electron radicals are expected to have significantly smaller reorganization energies, and their 16-electron cationic precursors are predicted to favor electron transfer in ion-pair annihilation under conditions of comparable driving forces. For example, see: Burke, M.; Brown, T. L. *J. Am. Chem. Soc.* **1989**, *111*, 5157.
(82) Marcus, R. A. *J. Chem. Phys.* **1956**, *24*, 966. For a review, see: Cannon, R. D. *Electron-Transfer Reactions*; Butterworths: London, 1980.
(83) See Figure 9 in: Fukuzumi, S.; Wong, C. L.; Kochi, J. K. *J. Am. Chem. Soc.* **1980**, *102*, 2928.
(84) Kochi, J. K. *Angew Chem., Int. Ed. Engl.* **1988**, *27*, 1227.
(85) Shaik, S. S. *Acta. Chem. Scand.* **1990**, *44*, 205.
(86) King, R. B.; Manuel, T. A.; Stone, F. G. A. *J. Inorg. Nucl. Chem.* **1961**, *16*, 233.
(87) (a) Pearson, A. J.; Kole, S. L.; Chen, B. *J. Am. Chem. Soc.* **1983**, *105*, 4483. (b) Burton, R.; Pratt, L.; Wilkinson, G. *J. Chem. Soc.* **1961**, 594.
(88) Kuchynka, D. J.; Amatore, C. A.; Kochi, J. K. *J. Organomet. Chem.* **1987**, *328*, 133.

and, after concentration to 5 mL, at −78 °C for 24 h afforded 48 mg pale yellow needles and 72 mg of very fine yellow needles, respectively. These were identified as *exo,exo,trans-* and *exo,-exo,cis*-5,5′-bis[(η^4-1,3-cyclohexadienyl)iron tricarbonyl], **6a**, in 30% and 45% yield respectively, identified from their IR and NMR spectra. Extraction of the red residue with 30 mL of CH_3CN at −20 °C to remove the $PPN^+PF_6^-$ gave 131 mg (0.267 mmol, 73%) of a purple powder, identified as $[CpMo(CO)_3]_2$, **7**.[17] IR (THF): ν(CO) 2011 (w), 1958 (vs), 1913 (s, br) cm^{-1}. ^1H NMR (CD_3NO_2): δ 5.45 (s, Cp). 5,5′-Bis[(η^4-cyclohexadienyl)iron tricarbonyl], **6a**,[19] trans isomer. ^1H NMR ($CDCl_3$): δ 5.31 (m, 4 H, H_2, $H_{2'}$, H_3, $H_{3'}$), 2.98 (m, 4 H, H_1, $H_{1'}$, H_4, $H_{4'}$), 1.90 (m, 4 H), 1.26 (m, 2 H, H_1, $H_{1'}$, 2 CH_2). IR (hexane): ν(CO) 2047 (s), 1981 (s) cm^{-1}. cis isomer. ^1H NMR ($CDCl_3$): δ 5.31 (m, 4 H), 3.03 (m, 4 H), 1.86 (m, 4 H), 1.11 (m, 2 H) (assignments same as trans isomer). ^{13}C NMR (C_6D_6): 212.5 (CO), 85.0 (C_2, C_3; split in $CDCl_3$), 65.3, 60.0 (C_1, C_4), 45.8 (C_5), 28.0 (C_6). IR (hexane): ν(CO) 2047 (s), 1981 (s) cm^{-1}.

Reaction of (η^5-cycloheptadienyl)Fe(CO)$_3^+$PF$_6^-$, 4, with PPN$^+$CpMo(CO)$_3^-$. To $PPN^+CpMo(CO)_3^-$ (52.1 mg, 0.067 mmol) suspended in 5 mL of THF was added 25.2 mg of (η^5-cycloheptadienyl)$Fe(CO)_3^+PF_6^-$, **4**. The mixture turned purple immediately and became homogeneous. The IR spectrum of the solution showed ν(CO) bands at 2043 (m), 2011 (w), 1970 (s), 1960 (vs), and 1913 (s) cm^{-1}. This spectrum corresponded to the complete formation of **7** together with **6b** [accompanied by a minor amount of (η^4-cycloheptadiene)$Fe(CO)_3$, as shown by TLC analysis (silica, hexane)].

Reaction of (η^5-cyclohexadienyl)Fe(CO)$_3^+$PF$_6^-$, 3, with PPN$^+$CpMo(CO)$_3^+$ at Low Temperatures. Addition of (η^5-cyclohexadienyl)$Fe(CO)_3^+PF_6^-$, **3** (67 mg, 0.185 mmol), to a suspension of $PPN^+CpMo(CO)_3^-$ (145 mg, 0.185 mmol) in 3 mL of THF at −78 °C gave a rapid color change to golden yellow. A cold mixture of 25 mL of ether/pentane (3:2 v/v) was added and the cold suspension filtered quickly. The yellow solution was concentrated in vacuo at −30 °C. The addition of 10 mL of cold hexane at <−50 °C and evaporation of the solvents in vacuo at −25 °C gave a pale yellow solid **8a**, which was unstable, even in the solid state at −18 °C. IR [Et_2O/hexane (1:2), −25 °C]: ν(CO) 2041 (s), 2010 (vs), 1971 (vs, br), 1927 (s, br), cm^{-1}. The product **8a** decomposed in solution [Et_2O/hexane (1:2)] at temperatures above −20 °C to afford a mixture of the two homo dimers **6a** and **7**. No intermediate was detectable. IR [Et_2O/hexane (1:2), 25 °C]: ν(CO) 2045 (s), 2011 (w), 1979 (vs), 1963 (s), 1919 (s) cm^{-1}.

Reaction between (η^5-cycloheptadienyl)Fe(CO)$_3^+$PF$_6^-$, 4, and PPN$^+$CpMo(CO)$_3^-$ at Low Temperatures. Addition of (η^5-cycloheptadienyl)$Fe(CO)^+PF_6^-$, **4** (15.1 mg (0.040 mmol), to 31.6 mg (0.040 mmol) of $PPN^+CpMo(CO)_3^-$ in 6 mL of THF at −78 °C gave a golden yellow solution. After 30 min at −78 °C, the solution was allowed to warm up, and a color change to red and then purple occurred at approximately −45 to −35 °C. No further color change occurred up to room temperature. The IR spectrum showed carbonyl bands at ν(CO) 2043 (s), 2011 (w), 1970 (s), 1961 (vs), and 1913 (s) cm^{-1}. This spectrum was attributed to a mixture of **7** and **6b**, together with minor amounts of (η^4-cycloheptadiene)$Fe(CO)_3$ and (η^4-cycloheptatriene)$Fe(CO)_3$ as shown by TLC analysis (silica, hexane).

Thermal Decomposition of the Nucleophilic Adduct 5a. A solution of **5a** (28 mg, 0.062 mmol) in 3 mL of hexane was kept at 50 °C overnight. The resulting suspension was cooled to −20 °C for 24 h. Removal of the red solid by filtration afforded 12.2 mg (0.025 mmol, 81%) of **7**. The mother liquor was filtered through a bed of silica. Concentration of the resulting yellow solution to 6 mL and cooling to −78 °C for 24 h gave 8.8 mg (0.021 mmol, 67%) of 5,5′-bis[(η^4-1,3-pentadienyl)tricarbonyliron], **6c**, as a pale yellow solid. The following IR, ^1H NMR, and ^{13}C NMR spectra showed it to be a mixture of two isomers.[31] **6c**. IR (hexane): ν(CO) 2051 (s), 1985 (s), 1975 (s) cm^{-1}. ^1H NMR (90 MHz, $CDCl_3$): δ 5.3–5.1 (m, 4 H, H_2, $H_{2'}$, H_3, $H_{3'}$), 1.8–1.6 [m, 6 H, 2 CH_2, H_1 (syn), $H_{1'}$ (syn)], 0.95 (m, 2 H, H_4, $H_{4'}$), 0.25 [dd, 2 H, H_1 (anti), $H_{1'}$ (anti)]. ^{13}C NMR ($CDCl_3$): δ 87.8, 81.6, 81.5 (C_2, $C_{2'}$, C_3, $C_{3'}$), 63.0 (C_4, $C_{4'}$), 39.7 (C_1, $C_{1'}$), 36.9, 36.3 (C_5, $C_{5'}$).

Thermal Decomposition of the Nucleophilic Adduct 5b. A solution of **5b** (21.1 mg, 0.0453 mmol) in 3 mL of hexane was kept in the dark at room temperature for 36 h. It was then cooled to −20 °C for 48 h, and the purple crystals, identified as $[CpMo(CO)_3]_2$, **7** (0.0203 mmol, 90%), were removed by filtration. The mother liquor was passed through a bed of silica. Concentration in vacuo afforded a yellow solid, identified as an isomeric mixture of bis[(η^4-hexadienyl)iron tricarbonyl], **6d** (0.020 mmol, 88%).[12b] IR (hexane): ν(CO) 2051 (s), 1987 (s), 1975 (s) cm^{-1}. ^1H NMR ($CDCl_3$): δ 5.2–5.0 (m), 1.7–1.3 (m), 1.1–0.8 (m), 0.4–0.1 (m) with relative intensities 2:3:3:1. The amount of **6d** (0.020 mmol) was determined by integration of the NMR signal at δ 5.2–5.0 (corresponding to 2 inner protons of the diene fragment) against the CH_2 protons of 9-(CH_2OH)-anthracene, added as internal standard. To ensure accurate measurement, a 10-s pulse delay was used.

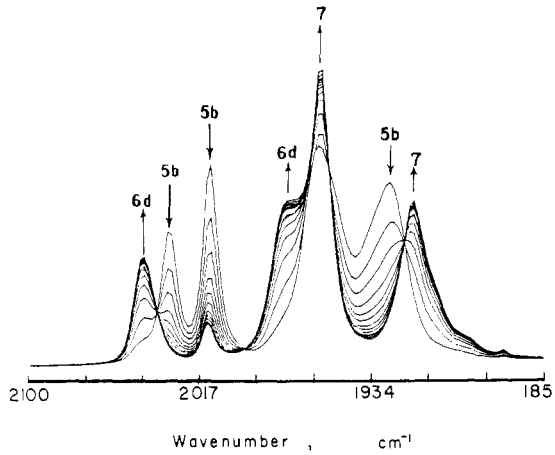

Figure 7. IR spectral changes accompanying the decomposition of the nucleophilic adduct **5b** in THF at 50 °C to afford the iron and molybdenum homo dimers, **6d** and **7**, respectively.

Electron Spin Resonance Spectroscopy of the Radical Intermediates. A solution of the nucleophilic adduct in THF (2×10^{-2} M) was placed in a Pyrex ESR tube under an argon atmosphere. The temporal changes in the amplitude of the ESR spectrum were recorded as the temperature was slowly raised (monotonically), as indicated in Figure 4. The singlet signals at $\langle g \rangle$ = 2.044 and 2.041 with peak-to-peak line widths of ΔH_{pp} = 30 and 20 G from **5a** and **5b**, respectively, could not be further resolved.

The ESR spectra of the spin adducts T_1, T_2, and T_3 in Figures 5 and 6 were obtained from 4.8×10^{-3} M nucleophilic adduct **5b** and 4×10^{-2} M 2-nitroso-2-methylpropane (NB) that was prepared in THF solution at 0 °C. The spectra of T_1 and T_2 were observed when the temperature of the solution was raised to 20 °C and persisted for several hours (see Figure 5). The resolved spectrum in Figure 6 was obtained 3 h later. The computer-simulated spectrum of the $m_I = 0$ line was obtained with the following parameters: a_N = 14.8 G, a_H = 1.15 and 0.47 G, and a_{Me} = 0.26 G.[89]

Determination of the Kinetics and the Products of Homolysis. The solvent (5 mL) contained in a Schlenk tube (equipped with Teflon valves) was initially equilibrated in a constant temperature ($\Delta T = \pm 0.5$ °C) oil bath kept in the dark to minimize its exposure to adventitious light. A weighed amount ($\sim 3 \times 10^{-2}$ mmol) of the nucleophilic adduct **5b** was added under a reverse stream of argon, and aliquots of the solution were periodically extracted for IR analysis. Complete reaction was ascertained after a minimum of 6 half-lives. The first-order rate constants in Table II were obtained by plotting the absorbance (D) change, i.e., $-(\ln [(D_t - D_\infty)/(D_0 - D_\infty)])$, versus time (min) for the nucleophilic adduct **5** and the homo dimers **6** and **7** at their characteristic carbonyl bands (vide supra). The similar procedure was used for homologue **5a**, but high conversions were precluded by the long times for thermolysis in competition with the competing decomposition of **7**. Careful spectral analysis indicated that only the homo dimers and no other products were formed from both **5a** and **5b** (e.g., see Figure 7).

The rate constants in Table III were obtained in the same manner as described above. Except for the dissolution of the

(89) We thank R. Sustmann (Essen) for kindly providing us with the ESR simulation program.

adduct in the solvent prior to the addition of **5**, the reactions in Table III were also carried out in 5 mL of THF (unless stated otherwise) at 31 °C. The spectral results were given as additive (concentration), k_H (10^3 s^{-1}); IR (THF, ν(CO), cm^{-1}): (i) $HCCl_3$ (2.1 M), 0.25; 2044 (m), 2011 (w), 1973 (s), 1958 (s), 1913 (m, br). (iia) CCl_4 (2.1 M), 1.20; 2051 (s, br), 1973 (s, br). (iib) CCl_4 (0.11 M), 1.04; 2051 (s, br), 1973 (s, br). (iii) $HCBr_3$ (0.32 M), 1.24; 2047 (s), 1969 (s, br). (iva) $HCBr_3$ (1.6 M, in hexane), 1.69; 2083 (m), 2053 (s), 2039 (m), 2003 (m), 1984 (vs), 1964 (s).[90] (ivb) $HCBr_3$ (0.32 M, in hexane), 1.58; 2083 (w), 2054 (s), 2038 (w), 2003 (w), 1985 (vs), 1964 (s).[90] (v) CBr_4 (0.07 M), 1.62; 2047 (s, br), 1969 (vs, br). (vi) $(CH_3)_3CNO$ (0.048 M), 1.08; 2045 (m), 1978 (m), 1966 (sh), 1940 (s), 1835 (s). (vii) PPh_3 (0.018 M), 0.85, and PPh_3 (0.04 M), 0.6; the complex mixture was separated by silica chromatography to afford **9** [IR (hexane): ν(CO) 1983 (vs), 1929 (s) cm^{-1}][91] and $Cp_2Mo_2(CO)_5PPh_3$ [IR (CCl_4): ν(CO) 1972 (s), 1895 (s, br), 1824 (m) cm^{-1}].[39] The structures of the products were assigned on the basis of the IR spectrum taken in hexane of the evaporated reaction mixture. **6d**. IR: ν(CO) 2051 (s), 1987 (s), 1975 (s) cm^{-1}. $CpMo(CO)_3Cl$. IR: ν(CO) 2057 (s), 1987 (vs), 1964 (s) cm^{-1}.[43] $CpMo(CO)_3Br$. IR: ν(CO) 2053 (s), 1984 (vs), 1964 (s) cm^{-1}.[41] Dimer **7** was assigned on the basis of its carbonyl bands at 2012 (w), 1956 (vs), and 1912 (s, br) cm^{-1} in the reaction mixture.[17]

Spectral Observation of the First-Formed Intermediates at Low Temperature. Separate solutions of $PPN^+CpMo(CO)_3^-$ (34.2 mg, 4.36×10^{-2} mmol) and $Fe(CO)_3L^+PF_6^-$ (4.36×10^{-2} mmol) each in 0.5 mL of acetone-d_6 were precooled to −78 °C. Upon mixing, the combined (equimolar) yellow solution was transferred to the precooled wide-bore spectrometer and the ^1H NMR spectrum measured at −35 °C. Similarly, yellow solutions were prepared in dichloromethane (1×10^{-3} M) for the measurement of the UV–vis and IR spectra at −60 °C. The 2-dimensional ^1H COSY spectra were measured by the standard pulse sequence[92] (usually with P_2 = 14 μs, D_5 = 700 ms, D_8 = 100 μs, and I_8 = 427 μs) with the central resonance of the solvent at 2.04 ppm as the internal reference. The first-formed intermediate A was observed as a clear yellow solution with the following spectral parameters. ^1H NMR (300 MHz, acetone-d_6, −35 °C): δ 5.59 (s, 5 H, Cp), 5.44 (dd, 1 H, H_4), 5.24 (dd, 1 H, H_3), 3.57 (ddd, 1 H, H_2), 2.99 (dq, 1 H, H_5), 2.31 (dd, 1 H, $H_{1'}$), 1.99 (dd, 1 H, H_1), 1.47 (d, 3 H, CH_3), 8.0–7.5 (m, 30 H) due to PPN^+. From the COSY spectrum: $J_{1,1'}$ = 9.3, $J_{1,2}$ = 13.5, $J_{1',2}$ = 4.0, $J_{2,3}$ = 7.2, $J_{3,4}$ = 5.1, $J_{4,5}$ = 9.3, $J_{5(CH_3)}$ = 6.3 Hz. IR (CH_2Cl_2, −35 °C): ν(CO) 2033 (vs), 2008 (vs), 1960 (vs, br), 1918 (s, br) cm^{-1}. UV–vis (CH_2Cl_2, ≅ 20 °C): λ_{max} = 340 nm (ε 10^4 M^{-1} cm^{-1}). Thus, the ^1H NMR spectrum observed at −35 °C clearly showed that a single compound was formed with one singlet for the Cp ligand of the molybdenum fragment and one methyl group plus six signals, each with the relative intensity of one, to account for every proton of an (hexadiene)$Fe(CO)_3Mo(CO)_3Cp$ isomer of **5b** (see Figure 1). Most importantly, the similarity of the IR spectra of A and **5b** mirror the information provided by the COSY spectrum for the protons H_1, $H_{1'}$, H_3, H_4, CH_3, and Cp that are almost identical in A and **5b** with $\Delta\delta < 0.1$ ppm. On the other hand, H_2 and H_5 are shifted downfield by 1.57 and 1.52 ppm, respectively, in a manner similar to that previously observed in a series of structurally related $Fe(CO)_3$(diene) complexes, in which H_2 and H_5 of the cis-substituted derivatives were consistently formed to resonate at lower fields, typically $\Delta\delta \cong 2.5$ ppm for H_2 and 1.0 ppm for H_5.[48] Finally, the significantly reduced value of $J_{2,3}$ in A relative to **5b** (compared to the invariance of $J_{4,5}$) completed the structural assignment given.

The thermally labile intermediate A when warmed to >−20 °C afforded an intensely red solution accompanied by significant changes in the carbonyl region of the IR spectrum to ν(CO) 2033 (m), 2008 (m), 1976 (vs), 1960 (vs, br), 1918 (m), and 1883 (m, br) cm^{-1}. The ^1H NMR spectrum showed that three compounds, B, C, and **5b**, were produced from A in an initial molar ratio of 2:1:1. The ratio of B:C remained more or less constant up to ~80% conversion of A, as **5b** gradually became the dominant species. After the thermal equilibration of the solution at room temperature, the ^1H NMR spectrum showed **5b** to be present in ~85% yield, together with **7** (~15% judging by the Cp resonance at 5.47 ppm). Similarly, the UV–vis spectrum of the equilibrated solution showed a shoulder at 370 nm together with a weak but significant absorbance with λ_{max} = 505 nm, both assigned to **7**.[93] Homo dimer **6c** was detected in the IR spectrum as shoulders at ν(CO) 2044 (w, sh) and 1975 (w, sh) cm^{-1}. The spectral changes accompanying the disappearance of A were characterized by the growth of a broad absorption band centered at λ_{max} 470 nm in the UV–vis spectrum (responsible for the observed red color), and the rapid disappearance of the carbonyl band ν(CO) 2010 cm^{-1} (characteristic of the Mo–C σ-bond[15]) and concomitant growth of a new band at 1883 cm^{-1} in the IR spectrum. Intermediates B and C were characterized by their distinctive ^1H NMR (COSY) spectra as follows. ^1H NMR (300 MHz, acetone-d_6, −35 °C, intermediate B): δ 5.95 (dq, 1 H, H_5), 5.53 (s, 5 H, Cp), 5.25 (m, 1 H, H_4), 5.10 (m, 1 H, H_3), 4.10 (ddd, 1 H, H_2), 3.35 (br d, 1 H, $H_{1'}$), 3.05 (br d, 1 H, H_1), 1.65 (d, 3 H, CH_3), $J_{1,1'} < 2$, $J_{1,2}$ = 13, $J_{1',2}$ = 8, $J_{2,3}$ = 8, $J_{4,5}$ = 16, $J_{5(CH_3)}$ = 6.5 Hz. ^1H NMR (300 MHz, acetone-d_6, −35 °C, intermediate C): δ 5.64 (s, 5 H, Cp), 5.53 (m, 1 H, H_3), 5.33 (m, 1 H, H_4), 2.82 (m, 1 H, H_1), 2.25 (m, 1 H, H_2), 1.74 (br d, 1 H, $H_{5'}$), 1.57 (d, 3 H, CH_3), 0.58 (br d, 1 H, H_5), $J_{1(CH_3)}$ = 7, $J_{4,5}$ = 10, $J_{4,5'}$ = 7 Hz. The five signals of the principal intermediate B were assigned from the normal spectrum and the other two, H_3 and H_4, were observed in the COSY spectrum by cross peaks to H_2 and H_5, respectively. In addition, the cross peaks between H_1, $H_{1'}$, and H_2 as well as H_5 and the Me group were observed. The signals for H_1, $H_{1'}$, and H_2 (indicative of terminal π-allyl[94]) together with δ H_5 and $J_{4,5}$ (indicative of a free, trans-substituted double bond[94]) were comparable to those in the known syn-(η^3-pentadienyl)$Fe(CO)_3Br$ with (H_1) 3.13 (d, J = 13 Hz), ($H_{1'}$) 3.30 (d, J = 8 Hz), (H_2) 3.95 (ddd, $J = 13 \times 13 \times 8$ Hz), (H_3) 5.02 (dd, $J = 13 \times 9$ Hz); (H_4) 5.80 (ddd, $J = 9 \times 9 \times 17$ Hz); (H_5) 5.3 (dd, $J = 17 \times 1$ Hz).[51] Moreover, the magnitude of the vicinal coupling constant $J_{2,3}$ = 13 Hz for the anti proton compared with $J_{2,3}$ = 8 Hz for the syn proton in B (vide supra).[95] The presence of intermediate C was clearly indicated by the resolved singlet for Cp and the doublet for Me. Furthermore, the resonances for H_5, $H_{5'}$, H_2, and H_1 could be observed, and the COSY spectrum showed the cross peak of H_1 with Me, H_2 with H_3, and H_4 with H_5 and $H_{5'}$. The similarity of this spectrum with the ^1H NMR spectrum of **5a**, i.e., especially the very characteristic δ H_5, led to C as a σ-adduct with the molybdenum bound to the C-2 carbon atom of the hexadienyl ligand. Of the four possible isomers (cis or trans substituted, with two diastereomers in each case), the trans adduct was preferred based on the arguments similar to those presented for A.[47] The structural similarity of C to A and **6b** suggests that the major spectral changes in the conversion of intermediate A were associated with the growth and disappearance of iron–molybdenum intermediate B with λ_{max} = 470 nm (ε ~ 8000 M^{-1} cm^{-1} based on its maximal concentration of ~40%) in the UV–vis spectrum and carbonyl bands at ν(CO) 1976 (vs), 1960 (vs, br), and 1883 (m, br) in the IR spectrum.

Electrochemical Behavior of $Fe(CO)_3L^+$. The reduction of $Fe(CO)_3L^+PF_6^-$ was initially examined in a cyclic voltammetric cell (greaseless, all Teflon valves) at a platinum electrode in either acetonitrile or THF containing 0.3 or 0.1 M tetra-*n*-butylammonium hexafluorophosphate [TBAH, G. F. Smith Co. recrystallized from ethyl acetate and dried in vacuo at 100 °C]. Cations **1**–**4** all showed irreversible cathodic waves (E_p^c) at CV scan rates of 0.5 V s^{-1} (Table IV). Interestingly **4** showed a pair of anodic waves at E_p^a = 0.67 and 1.12 V on the return scan switched at −1.0 V. By contrast **1**, **2**, and **3** showed no comparable anodic behavior at potentials less positive than 1.0 V that are characteristic for the oxidation of iron–iron bound dimers (e.g., **11**). For

(90) The structural assignment (η^3-hexadienyl)$Fe(CO)_3Br$ was based on its similarity to (η^3-pentadienyl)$Fe(CO)_3Br$: see ref 40.

(91) The strong carbonyl bands at 1983 and 1929 cm^{-1} are similar to those found in the C–C-bonded dimer [(diene)$Fe(CO)_2PPh_3]_2$[19] and the corresponding monomer (diene)$Fe(CO)_2PPh_3$. [Pearson, A. J.; Raithby, P. R. *J. Chem. Soc., Dalton Trans.* **1981**, 884. Chaudhari, F. M.; Pauson, P. L. *J. Organomet. Chem.* **1966**, *5*, 73.]

(92) Bax, A.; Freeman, R.; Morris, G. J. *J. Magn. Reson.* **1981**, *12*, 164.

(93) Wrighton, M. S.; Ginley, D. S. *J. Am. Chem. Soc.* **1975**, *97*, 4246.

(94) (a) Fish, R. W.; Giering, W. P.; Marten, D.; Rosenblum, M. *J. Organomet. Chem.* **1976**, *105*, 101. (b) Lee, T.-W.; Liu, R.-S. *Organometallics* **1988**, *7*, 878. (c) Bleeke, J. R.; Hays, M. K.; Wittenbrink, R. J. *Organometallics* **1988**, *7*, 1417.

(95) See ref 94 and ref 40.

Table V. Atomic Coordinates (×10⁴) and Equivalent Isotropic Displacement Parameters (Å² × 10³)[a]

	x	y	z	U(eq)
Mo	1966 (1)	2042 (1)	1121 (1)	41 (1)
Fe	3560 (1)	2950 (1)	-1084 (1)	47 (1)
O(1)	4756 (3)	1486 (6)	1609 (2)	97 (2)
O(2)	1193 (3)	-1134 (4)	300 (1)	68 (1)
O(3)	1708 (4)	-927 (5)	2066 (2)	98 (2)
O(4)	6045 (3)	2551 (5)	-475 (2)	100 (2)
O(5)	4679 (5)	3084 (7)	-2234 (2)	143 (2)
O(6)	3025 (4)	6646 (5)	-916 (2)	99 (2)
C(1)	1352 (5)	4873 (6)	783 (2)	62 (2)
C(2)	1838 (5)	5015 (6)	1375 (2)	64 (2)
C(3)	1077 (5)	4056 (7)	1741 (2)	62 (2)
C(4)	90 (4)	3304 (6)	1373 (2)	64 (2)
C(5)	276 (5)	3818 (6)	775 (2)	63 (2)
C(6)	3753 (5)	1659 (2)	1429 (2)	59 (2)
C(7)	1521 (4)	-2 (6)	597 (2)	48 (2)
C(8)	1790 (5)	158 (7)	1721 (2)	63 (2)
C(9)	3279 (4)	2362 (6)	315 (2)	48 (2)
C(10)	2600 (2)	2302 (6)	-285 (2)	43 (1)
C(11)	2762 (4)	852 (6)	-669 (2)	52 (2)
C(12)	2317 (5)	956 (6)	-1274 (2)	58 (2)
C(13)	1724 (5)	2499 (6)	-1489 (2)	57 (2)
C(14)	1395 (5)	2761 (8)	-2149 (2)	79 (2)
C(15)	5077 (5)	2689 (6)	-708 (2)	64 (2)
C(16)	4239 (5)	2998 (8)	-1787 (2)	80 (2)
C(17)	3250 (4)	5210 (7)	-980 (2)	58 (2)

[a] Equivalent isotropic U defined as one-third of the trace of the orthogonalized U_{ij} tensor.

comparison, the authentic sample of homo dimer **6b** showed an irreversible wave at E_p^c = −2.36 V and E_p^a = 1.10 V, and the iron–iron dimer II showed the corresponding waves at E_p^c = −1.95 V and E_p^a = 0.72 V.

The bulk electroreduction of cation **4** (201 mg, 0.53 mmol) in 40 mL of acetonitrile containing 0.1 M TBAH was carried out galvanostatically at 25 mA (V_{init} = −0.4 V). The yellow solution gradually turned orange, and at ~50% conversion the iron–iron dimer **11** began to precipitate. The gradual decrease of the applied potential to −0.6 V finally resulted in an overall consumption of 49.6 C (0.97 e). IR analysis of the catholyte showed carbonyl bands at ν(CO) 2040 (s), 1970 (vs, br), and 1756 (m) cm⁻¹, with the characteristic bands of **4** absent. Filtration, followed by recrystallization from a mixture of dichloromethane and hexane, afforded red crystals of **11** [IR (MeCN): ν(CO) 1985 (vs), 1954 (sh), 1755 (s) cm⁻¹. IR (THF): ν(CO) 1983 (s), 1952 (w), 1765 (s) cm⁻¹][55] in roughly 30% yield. Extraction of the catholyte with hexane, followed by the concentration of the hexane extract in vacuo and crystallization of the residue from ethanol, afforded yellow crystals of **6b**, as identified by its TLC behavior and IR spectrum with ν(CO) 2047 (s) and 1980 (vs) cm⁻¹ in hexane.

Solvent Effects and Reactivity of Ion-Pair Intermediates. The facile conversion of the first-formed species A at low temperatures (−35 °C) was examined in acetonitrile and in a 2:3 v/v mixture of pentane/THF. The transformation in both solvents followed the characteristic color change from yellow to orange at −18 °C, to orange-red at −15 °C, and finally to the red color of intermediate B at −10 °C. Such a parallel behavior in media of widely differing polarity indicated that transformation of A to B (etc.) occurred by a non-ionic pathway. For comparison, the ion-pair reversion of A induced by triphenylphosphine did not occur in THF under conditions in which the phosphonium salt **10** was spontaneously formed at −20 °C in acetonitrile with ν(CO) 2053 (s), 1983 (s), 1898 (s), and 1782 (vs) cm⁻¹ (see eq 11).[96] Under similar conditions, the labile intermediates **8a** derived from (cyclohexadienyl)-Fe(CO)$_3^+$ formed an analogous phosphonium salt and CpMo(CO)$_3^-$ with ν(CO) 2060 (s), 1990 (s), 1898 (s), and 1782 (s) cm⁻¹. The pentadienyl cation **1** also formed the homologous intermediate A′ that suffered ion-pair reversion with added PPh_3 [IR (MeCN): ν(CO) 2059 (s), 1989 (s, br), 1898 (s), 1782 (vs, br) cm⁻¹.

X-ray Crystallography of the Nucleophilic Adduct 5b. A bright orange parallelepiped of **5b** having approximate dimensions 0.26 × 0.28 × 0.28 mm was mounted on a glass fiber in a random orientation on a Nicolet R3m/V automatic diffractometer. The radiation used was Mo Kα monochromatized by a highly ordered graphite crystal. Final cell constants, as well as other information pertinent to data collection and refinement, were as follows: space group $P2_1/n$ (monoclinic); cell constants a = 10.642 (2) Å, b = 7.658 (1) Å, c = 22.440 (4) Å, β = 93.44 (1)°, V = 1825 Å; molecular formula $C_{17}H_{14}O_6FeMo$; formula weight 466.10; formula units per cell Z = 4; density ρ = 1.70 g cm⁻³; absorption coefficient μ = 14.9 cm⁻¹; radiation (Mo Kα) λ = 0.710 73 Å; collection range 4° < 2θ < 50°; scan width $\Delta\theta$ = 1.30 + ($K\alpha_2$ − $K\alpha_1$)°; scan speed range 2.5–15.0 deg min⁻¹; total data collection 3199; independent data with $I > 3\sigma(I)$ 2435; total variables 245; $R = \sum||F_o| - |F_c||/\sum|F_o|$ = 0.025; $R_w = [\sum w(|F_o| - |F_c|)^2/\sum w|R_o|^2]^{1/2}$ = 0.025; weights $w = \sigma(F)^{-2}$. The Laue symmetry was determined to be $2/m$, and from the systematic absences noted, the space group was shown unambiguously to be $P2_1/n$. Intensities were measured by using the ω scan technique, with the scan rate depending on the count obtained in rapid prescans of each reflection. Two standard reflections were monitored after every 2 h on every 100 data collected, and these showed no significant decay. In reducing the data, Lorentz and polarization corrections were applied, as well an empirical absorption correction based on ψ scans of 10 reflections having χ values between 70 and 90°. The structure was solved by interpretation of the Patterson map, which revealed the position of the Mo atom. The remaining non-hydrogen atoms were located in subsequent difference Fourier syntheses. The usual sequence of isotropic and anisotropic refinement was followed, after which the non-diene hydrogens were entered in ideal calculated positions and constrained to riding motion, with a single-variable isotropic temperature factor. The diene hydrogens were located in a difference map and allowed to refine independently, with mild distance constraints. After all shift/esd ratios were less than 0.2, convergence was reached at the agreement factors listed above. No unusually high correlations were noted between any of the variables in the last cycle of full-matrix least-squares refinement, and the final difference density map showed a maximum peak of about 0.25 e/Å³. All calculations were made by using Nicolet's SHELXTL PLUS (1987) series of crystallographic programs. The final atomic coordinates and equivalent isotropic parameters are included in Table V.

Acknowledgment. We thank T. M. Bockman for numerous helpful suggestions and discussions, J. D. Korp for crystallographic assistance and the National Science Foundation, and Robert A. Welch Foundation and the Texas Advanced Research Program for financial support.

Supplementary Material Available: Tables listing bond distances, bond angles, and anisotropic displacement parameters (3 pages); a table listing observed and calculated structure factors for **5b** (12 pages). Ordering information is given on any current masthead page.

(96) The two high-frequency bands were due to the cation (see ref 49), and the two bands at low frequency arose from CpMo(CO)$_3^-$ (see ref 14a).